Front. Mater. Sci. 2023, 17(2): 230644
https://doi.org/10.1007/s11706-023-0644-x

REVIEW ARTICLE

Three-dimensional printing of biomaterials for bone tissue engineering: a review

Ahmed El-Fiqi (✉)

Glass Research Department, Advanced Materials Technology and Mineral Resources Research Institute, National Research Centre, Cairo 12622, Egypt

ABSTRACT: Processing biomaterials into porous scaffolds for bone tissue engineering is a critical and a key step in defining and controlling their physicochemical, mechanical, and biological properties. Biomaterials such as polymers are commonly processed into porous scaffolds using conventional processing techniques, e.g., salt leaching. However, these traditional techniques have shown unavoidable limitations and several shortcomings. For instance, tissue-engineered porous scaffolds with a complex three-dimensional (3D) geometric architecture mimicking the complexity of the extracellular matrix of native tissues and with the ability to fit into irregular tissue defects cannot be produced using the conventional processing techniques. 3D printing has recently emerged as an advanced processing technology that enables the processing of biomaterials into 3D porous scaffolds with highly complex architectures and tunable shapes to precisely fit into irregular and complex tissue defects. 3D printing provides computer-based layer-by-layer additive manufacturing processes of highly precise and complex 3D structures with well-defined porosity and controlled mechanical properties in a highly reproducible manner. Furthermore, 3D printing technology provides an accurate patient-specific tissue defect model and enables the fabrication of a patient-specific tissue-engineered porous scaffold with pre-customized properties.

KEYWORDS: 3D printing; biomaterial ink; printability; 3D printing technique; 3D printed scaffold; bone tissue engineering

Contents

Received January 11, 2023; accepted March 7, 2023

E-mail: dr.ahmed.elfiqi@gmail.com

1 Introduction

Processing biomaterials into porous scaffolds for a certain tissue engineering application is a critical and a key step in defining and controlling their physicochemical, mechanical, and biological properties [1]. The processing methods of biomaterials into porous scaffolds vary from the conventional processing methods such as solvent casting, salt leaching [2], thermally induced phase separation [3], gas foaming [4], freeze-drying [5], and electrospinning [6] to the more advanced three-dimensional (3D) printing processing techniques such as fused deposition modelling (FDM) [7], selective laser sintering (SLS) [8], stereolithography (SLA) [9], and inkjet printing (IJP) [10]. The selection of a specific processing technique relies on the type of the biomaterial (either metals, ceramics, polymers or composites), its physicochemical and mechanical characteristics as well as on the final indented application in tissue engineering [11]. The traditional processing techniques of biomaterials have shown unavoidable limitations and several shortcomings [12]. For instance, tissue engineered scaffolds with complex 3D geometric architecture mimicking the complexity of extracellular matrix (ECM) of native tissues and with the ability to fit into irregular tissue defects [13] cannot be produced using the conventional processing techniques [14]. 3D printing has recently emerged as an advanced processing technology which enables processing of biomaterials into 3D porous scaffolds with complex architectures and tunable shape to precisely fit into irregular and complex tissue defects [15–17]. 3D printing is a manufacturing technology for printing complex 3D structures through a layer-by-layer additive deposition of a printable material (ink) using 3D digital models created with computer-aided design (CAD). By combining 3D printing with modern imaging and CAD, it is possible to quickly and easily create scaffolds with unique and complex shapes. 3D printing techniques enabled manufacturing of highly precise and complex 3D porous scaffolds with well-defined porosity and well-controlled mechanical properties [18–20]. Furthermore, the use of CAD in 3D printing permits accurate patient-specific tissue defect model and enables fabrication of a patient-specific tissue engineered scaffold with a pre-customized and personalized architecture [21]. 3D printing has recently become a hot area of research and it is now the subject of in-depth study for the production of 3D scaffolds for bone tissue engineering. This review provides a main focus on the recent application of 3D printing techniques for processing of biomaterials into 3D printed porous scaffolds for bone tissue engineering.

2 Conventional techniques for biomaterials processing into porous scaffolds

2.1 Conventional techniques for processing of biopolymer porous scaffolds

The conventional techniques commonly used in processing biomaterials into porous scaffolds, such as salt leaching, gas foaming, freeze-drying, and electrospinning are illustrated in Fig. 1 [22–24]. In the salt leaching method, porous scaffolds are constructed by pouring a combination of a polymeric solution and a salt powder in a mould and then the mixture is left for drying via a solvent evaporation process (Fig. 1(a)) [25]. The dried scaffolds are soaked in water in order to dissolve salt granules and the porous structure is created once all of salt granules have been entirely removed from the polymer matrix [26]. The porosity of the scaffolds prepared by this method is limited to the size and distribution of the salt granules [2]. Whereas, in the gas-foaming method, interconnected pores are made by using a gas as a porogen either by pumping a gas from external source or by *in situ* gas generation (Fig. 1(b) [22]). So, a polymer inside a container is saturated with a high-pressure gas. Then by dropping the gas pressure quickly, nucleation and development of pores take place. The pore shape and pore size of the scaffolds fabricated by this method are greatly influenced by the manufacturing factors such as

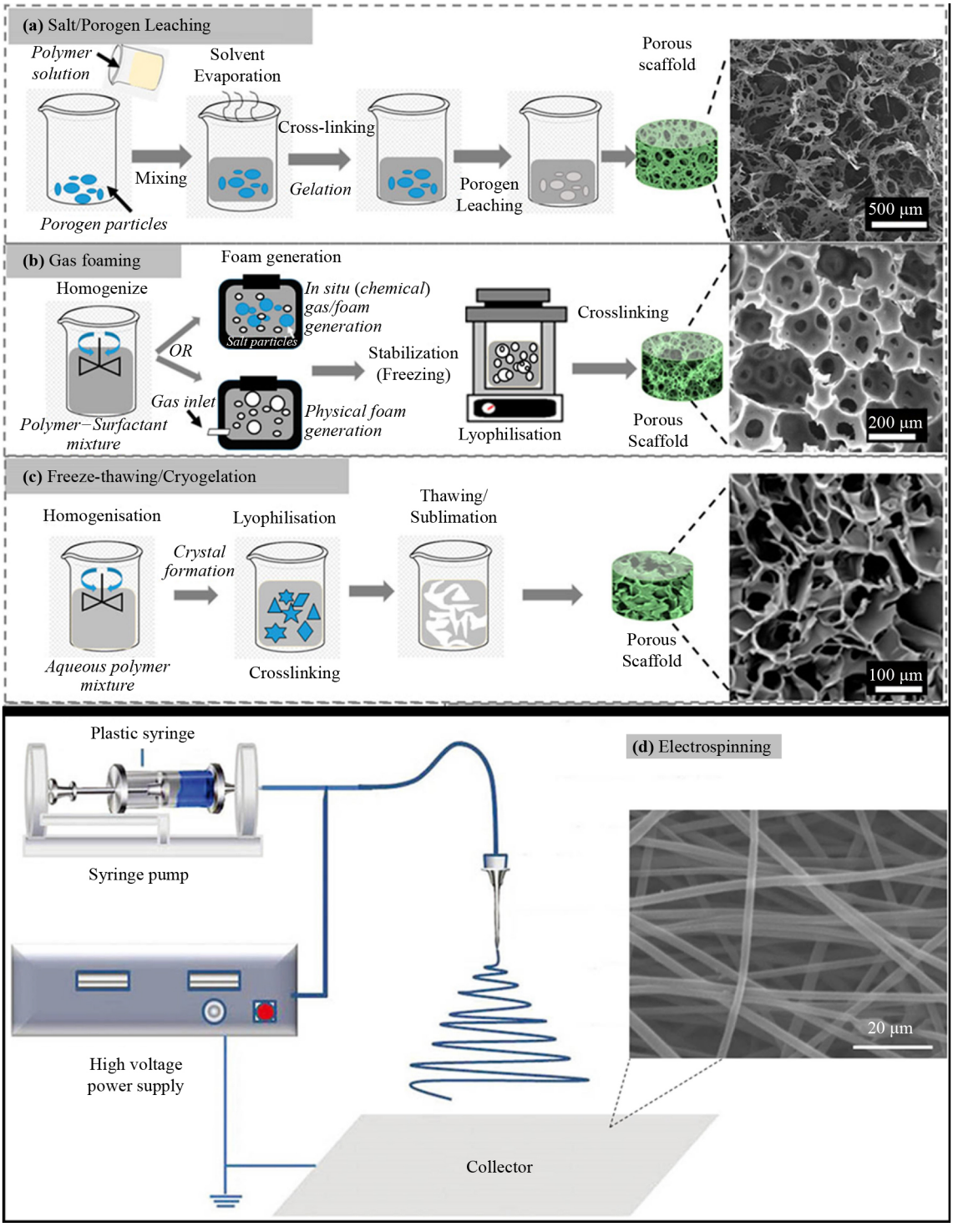

Fig. 1 (**a**)(**b**)(**c**) Illustrative diagrams for representative conventional techniques used in biomaterials processing into porous scaffolds. Reproduced with permission from Ref. [22] (Copyright 2021, Frontiers). (**d**) Schematic illustrations of electrospinning technique (this technique is limited to production of fibrous mats, i.e., 2D fibrous scaffolds, with limited thickness [23]). Reproduced with permission from Ref. [24] (Copyright 2017, John Wiley and Sons).

temperature, pressure, saturation level, and depressurization time. The scaffolds created by the gas-foaming method normally have an average porosity and appearance of a sponge [4].

Freeze-drying is another conventional processing method that involve casting of a polymer solution in a mould, and then freezing and drying it at low pressure. This process involves extracting the ice crystals by

sublimation (Fig. 1(c)) which leads to the formation of a porous scaffold [27]. Porosity of scaffolds prepared by freeze-drying is influenced by freezing rate, polymer amount, and processing temperature [5]. In the electrospinning process (Fig. 1(d) [24]), a polymer solution is pulled into fibres via electrostatic forces [23]. Syringe pump, power source, metal nozzle to pass electric current into polymer solution, and metal drum for fibre collection make up the four major components of an electrospinning machine [6,28]. A fibrous scaffold is formed as a result of the potential difference between the terminals, which leads to deposition of fibres on the metal collector [29–30]. The fibre diameter and morphology can be tailored by changing several parameters, e.g., polymer viscosity, applied electric field strength, polymer injection rate and type/speed of fibre collection (using either a static drum or a rotating drum). These conventional processing techniques are still widely applied in manufacturing of biomaterials-based porous scaffolds [31–38]. However, there are several drawbacks and unavoidable limitations (summarized in Table 1 [12]) revealed during their applications such as pore architecture, pore size uniformity, and pore network connectivity of porous scaffolds produced via salt leaching are challenging to manage [12,39]. Accordingly, non-uniform porosity, irregular pore size, non-uniform pore shape, low interconnectivity of pores network, long processing times and low reproducibility are commonly associated with the conventional processing methods [31]. Interestingly, 3D printing has recently emerged as an advanced processing technology that enables the processing of biomaterials into 3D porous scaffolds with highly controlled porosity and complex architecture [40]. The following sections are devoted to descriptions of 3D printing, 3D printing techniques, printability of biomaterials inks along with the application of 3D printing for bone tissue engineering.

2.2 Conventional techniques for processing of bioceramic and bioglass porous scaffolds

Bioceramic and bioglass porous scaffolds for tissue engineering can be produced using a variety of conventional processing methods. A few examples of these are sponge replica, sacrificial template (organic phase burning-out), and direct foaming methods, as schematically illustrated in Fig. 2 [41]. Each technique varies in producing a particular range of pore size, pore shape, pore interconnectivity, total porosity, strut thickness, and orientation.

In sponge replica method, a porous template made of a synthetic (usually a polyurethane (PU) sponge) or natural material (such as a marine sponge) is impregnated with a ceramic suspension (Fig. 2(a)). The excess slurry is then squeezed out of the sponge, allowing a thin layer of the slurry to be applied to the sponge struts. To create a porous ceramic with the same architecture as the sacrifice template, the coated template is pyrolyzed after drying while the leftover ceramic coating is sintered at higher temperatures (positive replica). As a result, the morphological traits of the ceramic foam are directly correlated with those of the polymeric template that was utilized. The sacrificial template method typically entails the creation of a biphasic composite made up of a continuous matrix of ceramic particles and a dispersed

Table 1 Limitations of conventional processing techniques (reproduced with permission from Ref. [12], Copyright 2018, Elsevier)

Manufacturing method	Benefits	Potential limitations
Solvent casting/particulate leaching	Relatively simple technique that allows creation of scaffolds with regular porosity, controlled composition and pore size	• Use of organic solvents precludes cells and biomolecules being included directly in scaffolds • Difficult to control pore shape and interconnectivity • Limited thickness of structures and mechanical properties achievable
Gas foaming	Eliminates use of chemical solvents	• High pressures involved prohibits inclusion of cells and bioactive molecules directly into scaffolds • Temperature labile materials may be denatured during compression moulding step • Difficult to control pore sizes and ensure interconnectivity
Emulsification freeze-drying	Does not require use of solid porogen	• Requires use of organic solvents • Small pore size • Porosity often irregular • Long processing time
Phase separation	• Eliminates leaching step of porogen • Can be combined with other techniques easily	• Small pore sizes limit its use • Use of organic solvents inhibits use of bioactive molecules or cells during scaffold fabrication
Electrospinning	• Creates scaffolds with large surface area for cell attachment • Simple and inexpensive technique	• Organic solvents may be required, which can be harmful to cells • Limited mechanical properties • Difficult to incorporate precise microarchitecture into constructs

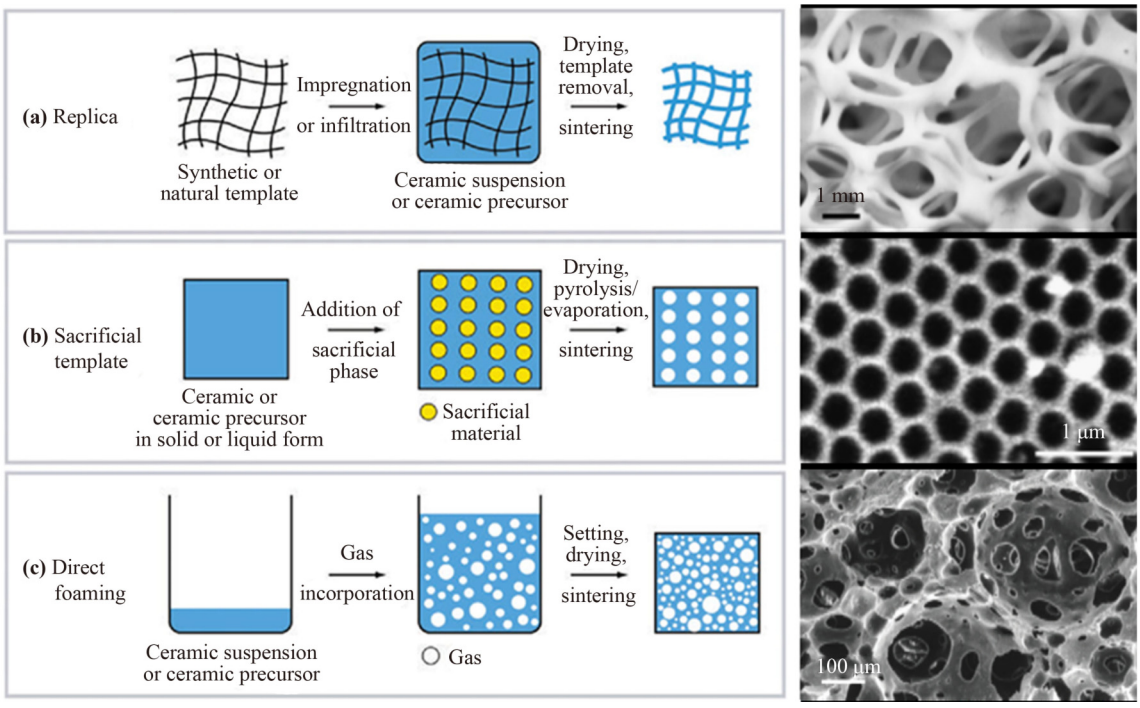

Fig. 2 Conventional processing routes used for the production of porous ceramic scaffolds: (**a**) replica; (**b**) sacrificial template; (**c**) direct foaming. Reproduced with permission from Ref. [41] (Copyright 2006, John Wiley and Sons).

sacrificial phase that is initially uniformly distributed throughout the matrix before being eventually extracted to create pores in the microstructure (Fig. 2(b)). Common methods for creating a biphasic composite include pressing a powder mixture of synthetic (e.g., poly (methyl methacrylate) or polyethylene microbeads) or natural origin (e.g., rice husk), and then, the mixture is thermally treated at a high temperature. When heated, the polymeric particles that fill the component's volume disintegrate, while the inorganic particles sinter, creating a porous body that shows a reversed version of the original sacrificial template [42]. Pore interconnectivity is typically minimal in scaffolds prepared by this method owing to the difficulties in maintaining a homogenous dispersion of the polymer spheres. In direct foaming methods, a gas in the form of bubbles can be dispersed into a ceramic suspension or colloidal sols, followed by solidification, to generate highly porous ceramics (Fig. 2(c)). There are several ways for the incorporation of gas bubbles into a ceramic suspension. For example, when using H_2O_2 as a foaming agent, ceramic powder is mixed with an aqueous solution of H_2O_2 before being cast into moulds and heated to 60 °C. At this temperature, H_2O_2 breaks down, and the oxygen that is released tends to create bubbles in the slurry, which starts the foaming process. The percentage of porosity and pore size can be controlled by changing the amount of H_2O_2 included and the heat treatment. Yet this foaming process has an inherent flaw in that pores are only joined in a laminar fashion, which leads to poor connectivity in the direction perpendicular to the laminae.

The *in-situ* polymerization (or gel-cast foaming) of an organic monomer can be used in place of H_2O_2 foaming. In gel-cast foaming, an organic monomer that must be soluble in water (like acrylates) is combined with an initiator and a catalyst to achieve in situ polymerization in a high-solid-load aqueous ceramic solution. To create a wet ceramic foam, the suspension is physically agitated after the addition of a surfactant, which acts as a foaming agent. A mold is then used to cast the foam, and once polymerization is finished, the green body can be withdrawn from the mold and placed in an oven to dry, burn out the polymer, and sinter the ceramic particles. The resulting ceramic foam obtained gel-cast foaming has better strength compared to other conventional procedures, However the porous structure is poorly connected and non-uniform.

Sol-gel foaming is another method that combines mechanical foaming with sol-gel synthesis method, a chemical-based wet synthesis procedure that transforms a ceramic precursor solution (sol) into a covalently bound silicate network (gel) by inorganic polymerization processes. A glass or glass–ceramic 3D scaffold with a

hierarchical structure, interconnected macropores can be obtained after heat treatment process [42]. The main steps in the sol-gel foaming are as follows: preparing a sol from precursor solutions, followed by foaming through vigorous agitation along with the addition of a gelling agent, a surfactant, then casting and gelation of the foamed sol mixture, finally, removing the solvent by drying at a low temperature, and sintering to produce a porous scaffold. An unavoidable limitation of sol-gel foaming method is the scaffold's inherent brittleness (too low mechanical strength caused by its nanoporous texture) which is an inescapable constraint that causes serious problems for the scaffold's safe *in-vivo* implantation. Comparison of a variety of conventional processing methods for bioceramic and bioglass porous scaffolds based on their benefits and drawbacks is given in Table 2 [42].

3 3D printing for biomaterials processing into porous scaffolds

3D printing is a manufacturing technology for printing complex 3D structures through a layer-by-layer additive deposition of a printable material (ink) using 3D digital models created with CAD [43]. By combining 3D printing with modern imaging and CADs, it is possible to quickly and easily create scaffolds with unique and complex shapes. The unique merits exhibited by 3D printing technology includes high flexibility in design, high ability to manufacture complex 3D architecture, high precision and accuracy, high reproducibility, rapid fabrication process and low waste production [44]. The exact control over scaffold exterior form, internal architecture, porosity, pore design, pore size, and pore network interconnectivity that 3D printing techniques can provide is impossible to achieve using conventional methods. Thus, a potential merit that 3D printing offers over conventional processing techniques is the ability to design porosity and complex architectural features. Porosity, pore size, pore shape, and pores network connectivity are highly important parameters for tissue engineering scaffolds. Actually, porosity allows diffusion of nutrients and oxygen to cells and enables cell migration, cell proliferation, and provides enough space for tissue vascularization. Moreover, pore size and pore shape can significantly affect cells distribution within the scaffold therefore, pore size and pore shape must be well-designed [43,45]. Figure 3 shows an illustrative design of a biomaterial 3D printer along with 3D printed porous scaffolds with well-controlled porosity [46–47].

Additionally, 3D printing enables processing of biomaterials into customized porous scaffolds to precisely fit into irregular and complex tissue defects [8,21,40]. Furthermore, the involvement of CAD in 3D printing technology permits accurate patient-specific tissue defect model and enables fabrication of patient-specific 3D printed porous scaffolds with a pre-customized and personalized architecture [8,21,40] as illustrated in Fig. 4 [8,21,48].

The use of a wide range of 3D printing techniques enabled the production of 3D structures with complex architectures and unique shapes. The 3D printing techniques relevant to processing of biomaterials into porous scaffolds are described in the following sections.

3.1 3D printing techniques

There are four main 3D printing processes (Fig. 5 [49]) that are utilized for transforming biomaterials into 3D

Table 2 Comparison of conventional processing methods for bioceramic and bioglass porous scaffolds (reproduced with permission from Ref. [42], Copyright 2015, Frontiers)

Technique	Advantages	Disadvantages
Foaming methods (general)	Allows manufacturing of both closed and open-cell foams; good versatility of final part shapes, as the solution can be cast in molds without additional machining	Difficulty in achieving high interconnectivity; non-porous external surface
H_2O_2 foaming	Simple	Low porosity control, laminar pore structure with poor 3D interconnection
Sol-gel foaming	Hierarchical structure can be obtained (macroporous scaffold combined with ordered mesoporous texture)	Need for a high degree of control of the foaming step
In situ polymerization of organic monomer (gel-cast foaming)	Highly porous ceramic; high-strength properties due to the less flawed structure and dense struts and walls produced	Low pore interconnectivity
Organic phase burningout/space holder	High mechanical strength	Difficult to obtain a homogeneous distribution of pores; poor interconnectivity
Sponge replication	Reticulated pen-cell material; applicable to any ceramic material that can be dispersed into a suspension; no toxic chemicals needed	Mechanical properties might be poor

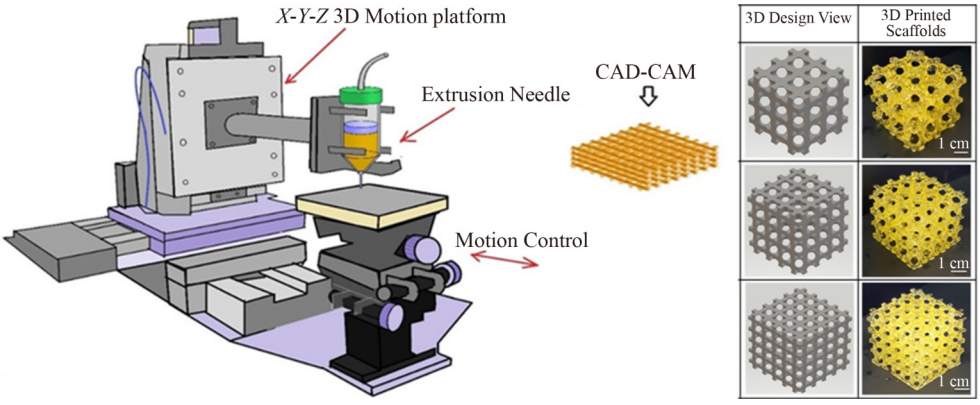

Fig. 3 Illustrative design of a biomaterial 3D printer (left) (reproduced with permission from Ref. [46], Copyright 2021, John Wiley and Sons). 3D printed porous scaffolds with well controlled porosity and pore size (right) (reproduced with permission from Ref. [47], Copyright 2022, The American Chemical Society).

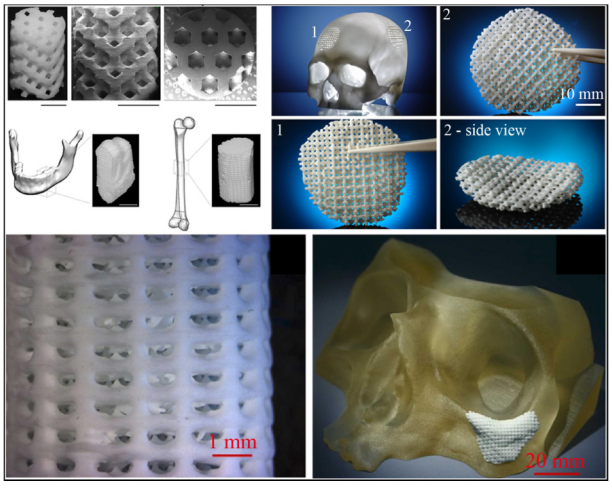

Fig. 4 Exemplary images of 3D printed patient-specific porous scaffolds with the same shape as the bone tissue defects: bioceramic (upper left) (reproduced with permission from Ref. [21], Copyright 2021, Elsevier); biopoymer (upper right) (reproduced with permission from Ref. [8], Copyright 2019, Elsevier); bioglass (lower panel) (reproduced with permission from Ref. [48], Copyright 2012, Elsevier).

printed porous scaffolds: SLS, SLA, FDM, and IJP. Light-based methods include SLS and SLA [43]. Light is used to sinter powdered materials in selective laser sintering and SLA, as well as to photopolymerize liquid materials into 3D structures. In SLA, a liquid resin must undergo photo-induced polymerization in the precise areas that are exposed to light [9]. While localized heating is provided by selective laser sintering to melt or fuse powder grains [8]. FDM involves ink extrusion and as ink travels through the nozzle of FDM printer, and it is thermally or chemically treated [7]. IJP relies on liquid intermediates or precursors that may quickly harden following ejection. IJP (also known as powder bed methods) involves binding powders on a *Z*-axial moving bed to produce 3D models [43]. These popular 3D printing techniques are illustrated in Fig. 5. The working principle, main characteristics, processing parameters, advantages, and disadvantages of each technique are described in the following sections.

3.1.1 Stereolithography (SLA)

An aqueous photocurable polymer is exposed to ultraviolet (UV) laser radiation during SLA as illustrated in Fig. 5 [49]. The light source projects a pattern of laser onto the liquid substance in order to harden the exposed area. The SLA printer uses an aqueous photocurable polymer as the raw material and continues the process after the first layer of the scaffold has solidified. Complex 3D structures can be printed using a laser source, a photopolymer, and a printing platform [21]. Only a few biomaterials can be employed in SLA since it needs a photosensitive material to print constructions. SLA is renowned for its high degree of accuracy and capacity to build extremely porous interconnected systems. Several factors have been considered while fabricating scaffolds using the SLA technology to influence their shape and mechanical characteristics [43] including the orientations of the construction parts as well as the printer settings, printing parameters, and material-related parameters (Fig. 6 [50]). Lack of a variety of biocompatible photocurable biomaterials is considered a drawback of this technique. Laser power, scan speed, scan pattern, layer thickness, and resin properties are significant SLA parameters.

With a resolution of about 50 µm, SLA is a reasonably

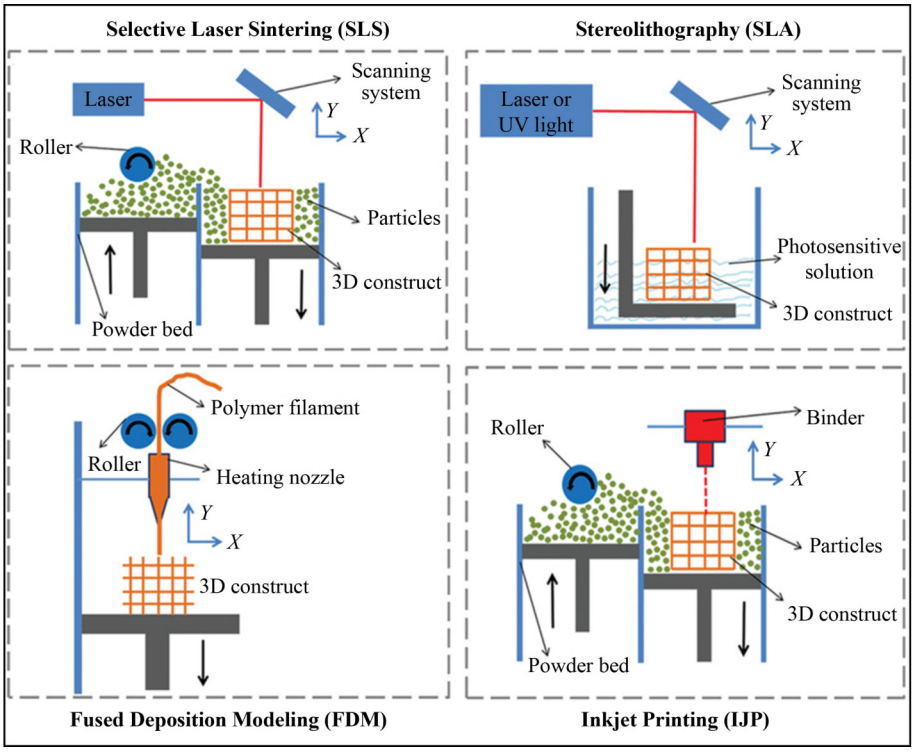

Fig. 5 3D printing techniques common for processing of biomaterials into 3D printed porous scaffolds. Reproduced with permission from Ref. [49] (Copyright 2020, John Wiley and Sons).

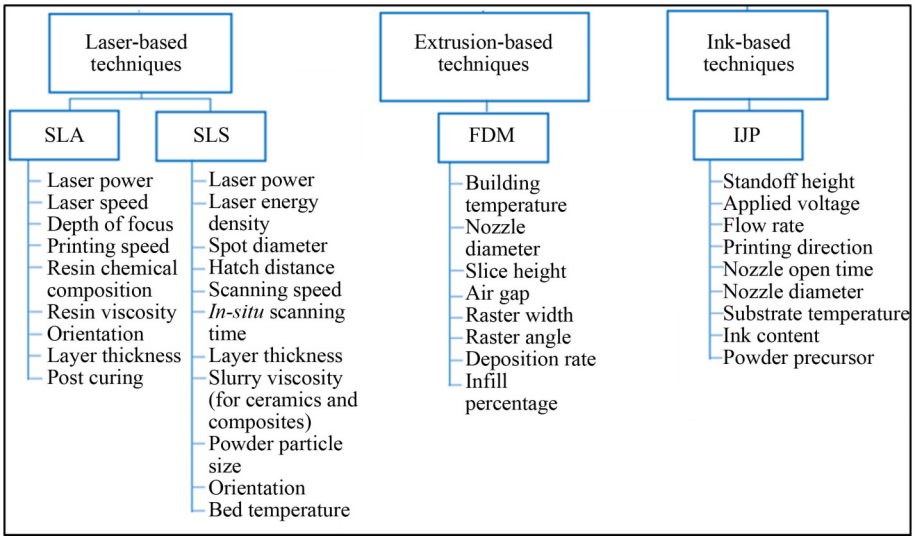

Fig. 6 Parameters and variables affecting 3D printing techniques. Reproduced with permission from Ref. [50] (Copyright 2020, Springer Nature).

rapid process that can create scaffolds with exact internal architecture and geometries. SLA also makes it possible to manufacture scaffolds with clearly defined porosities, pore size distribution, interconnectivity, and gradients [51]. One drawback is that it is inherently more expensive than alternative methods. Additionally, inorganic fillers may cause sedimentation in the photopolymer, which might cause problems with homogeneity that could influence the final structure and perhaps prevent photopolymerization [43]. Collectively, SLA is a revolutionary 3D printing technique used mostly with photopolymers to create very precise objects. However, SLA is a time-consuming technique with a difficult procedure and it can only be used with specific materials.

3.1.2 Selective laser sintering (SLS)

SLA and SLS printing methods are relatively similar, although SLS employs a powder material form (mostly a polymer) rather than a liquid one. SLS, often referred to as powder bed fusion, uses a focused laser to locally fuse or sinter the powdered material by heating it over its melting temperature [52]. The laser repeatedly fuses each patterned layer to produce 3D objects. The precision of printed objects is merely affected by the laser source resolution and ink grain size. One of SLS's most productive uses in bone tissue engineering is sintering composite biomaterials. The powder bed makes it feasible to print overhanging geometries, which gives the technology the potential to sustain complex printed structures on its own. SLS is a process that fuses powder into 3D objects with resolutions between 20 and 50 μm using a laser beam. The shape, particle size distribution, and flowability of the used powder are important factors in SLS. As shown in Fig. 6 [50], various parameters can be taken into account when fabricating scaffolds using SLS including printer and printing parameters, material characteristics, and orientation of the construction component [43]. To optimize the scaffold's morphology and mechanical characteristics, further factors need to be monitored including powder particle size, laser power, scan distance, scan speed, layer thickness, and part bed temperature. By altering these processing settings, the SLS technology offers great benefits for producing complex structures [40,44].

SLS offers several advantages over other 3D printing techniques including speed, the ability to print large objects and intricate structures, in addition to the presence of a powder bed that supports the building structure and enables the creation of overhangs. The disadvantage of this approach is that because the sintering process requires high temperatures, it cannot incorporate cells or biomaterials that are temperature-sensitive. Additionally, SLS-made scaffolds have a rough, porous surface and rather poor mechanical properties. Both SLM and SLS are comparable processes, however SLM is frequently used for metals and alloys like titanium and titanium alloys [15,53].

3.1.3 Fused deposition modelling (FDM)

FDM is a 3D printing technique that performs melting of a material mostly a thermoplastic polymer along with its extrusion through a moveable nozzle. Extrusion is accomplished by using mechanical or air pressure and can be adjusted by the pressure applied, the printing speed, the nozzle size, and the processing temperature [7]. The nozzle moves in X and Y along with Z directions to print each layer in a scaffold as illustrated in Fig. 5. Printed layers solidify and get bonded to each other, thus making a 3D scaffold. When using the FDM process for the production of the scaffold, numerous variables must be taken into account as listed in Fig. 6. Furthermore, changing the printing speed allows easy modification of the porosity and other features [43,54]. As an established 3D printing technique in tissue engineering, FDM is affordable, cost-effective, safe (no use of organic solvents), simple to use (post-processing is rarely necessary), and fast technique [54]. Also, FDM has the benefit of functioning as a desktop 3D printing facility in a design workplace. The most popular materials used in FDM are affordable, nontoxic, odorless, and ecologically secure [55]. However, FDM cannot be used to print certain biomaterials due to the high temperature employed during printing. Furthermore, FDM as an extrusion-based 3D printing technique has the drawback that its resolution, 200–500 μm, is very poor when compared to other techniques.

3.1.4 Inkjet printing (IJP)/binder jetting (BJ)

Another potential 3D printing technique, known as IJP or BJ, is frequently employed in tissue engineering to create intricate, high-resolution (<100 μm) constructs [10]. Low-viscosity binder solution droplets are selectively deposited from an inkjet head that follows the CAD file's X-Y movement instructions.

The binder aids in "glueing" the particles together and is selectively deposited at the powder bed. Although, composition of the binder and the droplet size must be tuned to produce components of high quality, BJ is of special interest in biomedical applications because of its room temperature processing and versatility in printing ceramic and polymer scaffolds [43]. A good manufacturing of a 3D scaffold by IJP requires several factors to be optimized as listed in Fig. 6. IJP is hence a quick and affordable technique, however, the scaffolds created by IJP are frequently brittle and need to be strengthen by post-processing treatments. Finally, the IJP technique is simple to utilize in bone tissue engineering because of its great flexibility in printing many types of materials

including ceramics, polymers, and ceramic/polymer composites in addition to biomaterials with cells (bioink) [56]. The accuracy, cost, advantages and disadvantages of each 3D printing technique are compared in Table 3 [57].

3.2 Biomaterials inks and printability requirements

Inks of polymers and composite biomaterials are widely applied in 3D printing because these inks can be cross-linked by various methods which make them easily printable. The printability requirements are dependent on the 3D printing technique, for instance, the printability requirements for biomaterial inks used in IJP are different from the printability requirements for extrusion-based printing. Generally, the phase transition of a biomaterial ink from a liquid to a solid state is an essential factor for a biomaterial to be printable. Among key factors that affect biomaterials inks printability are the method of ink cross-linking and ink rheological properties [58]. The biomaterial inks can be physically or chemically cross-linked. The liquid to solid phase transition mechanism defines the speed, fidelity and resolution of the biomaterial ink printability [59]. For example, physically cross-linked biopolymer hydrogels (e.g., by using pH changes) are mechanically weak (cross-linked through hydrogen bonds). Whereas, chemically cross-linked biopolymer hydrogels (e.g., by using a chemical cross-linker) are mechanically strong (cross-linked through covalent bonds) and have a good printability. Rheological properties, e.g., viscosity, viscoelastic behavior, and shear thinning, are determinant factors in biomaterials inks printability. For example, inks with shear thinning and non-Newtonian flow possess a good printability because they become less viscous when exposed to shear pressures and they have time-independent viscosity [59]. Whereas, a shear thickening ink become more viscous under pressure and it is more likely to block the printer needle. Figure 7 [58,60] shows a schematic illustration of the flow of a biomaterial ink inside the printing needle and the formation of first printed layer of filament on the

Table 3 Comparison of different 3D printing techniques (reproduced with permission from Ref. [57], Copyright 2021, AIP Publishing)

3D printing technique		Typical material	Resolution	Advantages	Shortcomings
Sort	Method				
Liquid-based 3D printing	Stereolithography (SLA)	Photo-curable polymer resins	50–100 μm	High resolution, smooth surface of fabricated structures	Over-curing, which can cause overhanging parts, oxygen inhibition, brittle printed products
	Digital light projection (DLP)	Photo-curable polymer resins	10–50 μm	High printing speed, less affected by oxygen inhibition than SLA	Requiring low viscosity resins, limited mechanical properties of the printed products
	Inkjet printing (IJP)	Polymers, hydrogels	50–300 μm	Relatively high printing speed (up to 10000 drops/s), low cost, allowing printing of bioinks containing living cells	Limited materials in a narrow range of viscosity (3.5–12 mPa·s), unable to fabricate large and complex structures
	Polyjet	Photo-curable polymer resins with very low viscosity and high surface tension	20 μm	High resolution, good surface quality of printed structures, relatively high printing speed, allowing fabrication of multi-lateral or multicolor objects	Very limited materials choices, expensive
Filament- or paste-based 3D printing	Fused deposition modelling (FDM)	Polymers and their composites in the filament form	100–150 μm	Robust, low cost, ability to process a variety of materials	Slow printing speed, relatively low dimension precision, requiring high temperature
	3D dispensing	Polymers, hydrogels, ceramics, and their composites	100 μm to millimeters	Ability to process a variety of materials in a wide range of viscosity ($(6–30)\times10^7$ mPa·s), capable of printing bioinks containing living cells	Printing nozzle clogging, rough surface of products, relatively low printing resolution
Powder-based 3D printing	Selective laser sintering (SLS)	Polymer powders, ceramic powders, and composite powders	50–100 μm	Relatively wide range of powder materials, fabrication of complex structures	Requiring high temperature, rough surface of products, low reusability of non-sintered powders
	Selective laser melting (SLM)	Polymer powders, ceramic powders, metal powders, and composite powders	20–100 μm	Ability to process metallic materials, near net-shape fabrication, high material utilization	Difficult to control printing, balling, high residual stress, deformation issues for printed parts
	Electron beam melting (EBM)	Metal powders	100–200 μm	High power electron energy source, faster printing speed than SLM	Lower resolution and rougher surface as compared to SLM
	3D powder binding (3DPB)	Polymer powders, ceramic powders, and their composite power	100 μm	Fast, low cost, allowing fabrication of multicolor objects	Low precision, rough surface, and limited mechanical strength of products

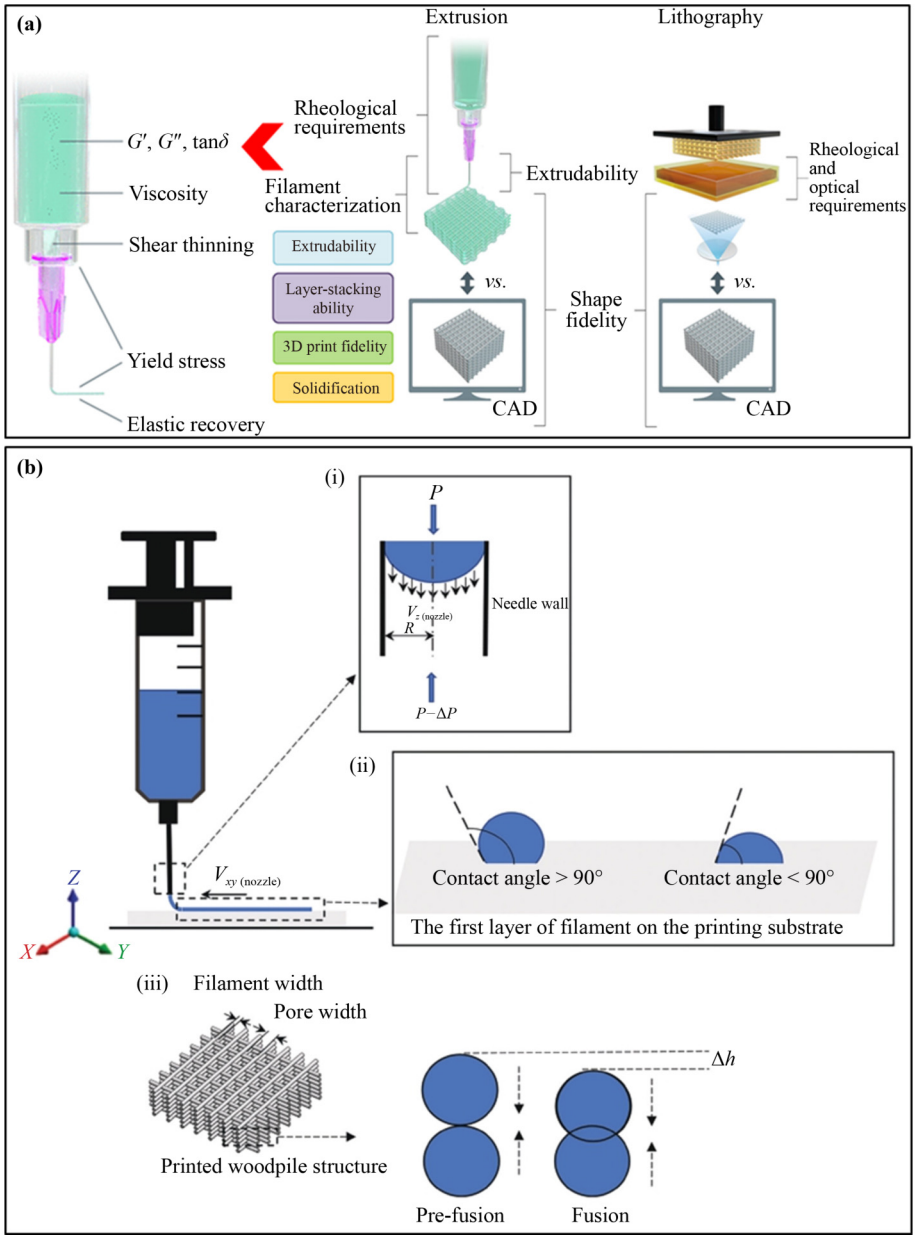

Fig. 7 (**a**) Rheological properties affecting printability and shape fidelity. Interplay of rheological properties in extrusion-based printing. Key aspects to assess printability in the context of extrusion- and lithography-based 3D printing technologies. Reproduced with permission from Ref. [61] (Copyright 2020, The American Chemical Society). (**b**) Illustration of a biomaterial ink flowability through the printing needle (i) and the formation of first printed layer of filament on the substrate (ii), and the vertical fusion of two filament layers within the 3D printed scaffold (iii). Reproduced with permission from Ref. [58] (Copyright 2020, Whioce Publishing).

substrate. Biomaterial inks can be cell-incompatible during 3D printing, whereas the 3D printed biomaterials are then subjected to post-printing treatments to render them cell-biocompatible prior to application. For example, biomaterial inks may contain cytotoxic organic solvents. However, these toxic solvents can be completely removed prior to encapsulation of cells and prior to *in-vivo* implantation. Furthermore, biomaterial inks can be subjected to high temperatures during 3D printing therefore incorporation of biomolecules/drugs and heat-sensitive components must be carefully considered prior to 3D printing process [61]. Biomaterial inks can also be combined with supportive inks to avoid their poor printability. Supportive inks can be temporary ink (removed from the printed material) or permeant ink (remains within the printed material).

In addition to supportive inks, viscous and/or hydrophobic plotting medium can be used to improve the

printability of biomaterial inks. However, removal of such plotting medium from the 3D printed material may complicate the fabrication process [58].

4 Application of 3D printed biomaterials for bone tissue engineering

4.1 Bone tissue

Bone is a highly specialized kind of connective tissue with excellent mechanical and biological capabilities. It is a complex organic–inorganic nanocomposite structure. It functions like a dynamic tissue due to the unique capacity of its osteoblasts, osteoclasts, and osteocyte cells to renew and remodel. However, when a bone defect is of a critical size, the injured tissue cannot be repaired by bone cells because the defect is too large. As roughly depicted in Fig. 8 [44], natural bone is structurally composed of inorganic carbonated apatite nanocrystals and collagen, a protein-based template. Apatite nanocrystals (about 100 nm) are encased among collagen fibres, which range in diameter from 50 to 500 nm. Native bone has extraordinary mechanical characteristics, including high resistance to tensile/compressive stresses, low stiffness, and high toughness, due to the unique formulation of the inorganic apatite phase with the elastic collagen hydrogel network. Bone cells, many soluble factors, and extracellular matrix elements are present throughout the cavities of bone and are continually active in the development and remodeling of bone [62].

4.2 Bone defects

Many inherited or congenital disorders can result in bony abnormalities. Congenital bone malformations are frequently caused by missing or improperly developing bones. Trauma, infection, tumour, or surgical removal are some of the common acute causes of acquired bone abnormalities. Over time, bone loss in weight-bearing sites is also a result of osteodegenerative illnesses such osteoarthritis. The number of individuals with these osteodegenerative diseases and the accompanying medical costs are anticipated to increase in both industrialized and developing nations due to an ageing population [63]. In orthopaedic surgery, bone defects continue to be a significant concern; Bone is the second most transplanted tissue in the world after blood, with an estimated 500000 surgeries needing bone grafts every year alone in the United States. Figure 9 illustrates and describes the common procedures utilized to treat bone loss due to accident or trauma [52]. Bone grafts are still the preferred therapy for these kinds of bone loss. The process of replacing missing or injured bones using tissue from the patient's own body, from donors, from animals, or both is known as bone grafting (xenografts). Autologous, allogeneic, or the use of bone graft replacements for the repair of significant abnormalities are currently the main regenerative therapeutic options for bone defects. Considering that the bone taken from the patients themselves includes live cells and growth hormones, autograft is still regarded as the gold standard today. However, there are a few drawbacks of autograft,

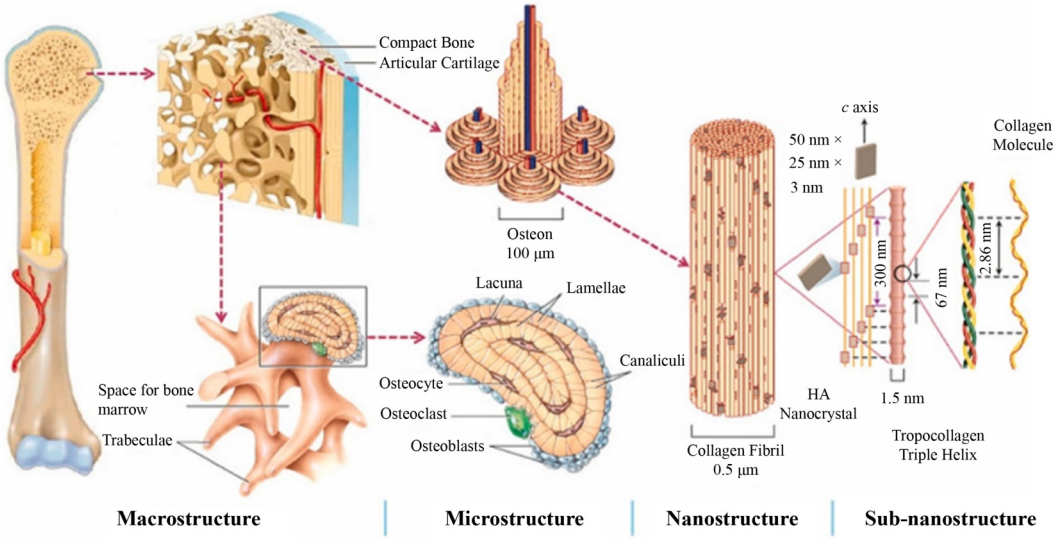

Fig. 8 Hierarchical structural organization of the bone tissue. Reproduced with permission from Ref. [44] (Copyright 2021, Elsevier).

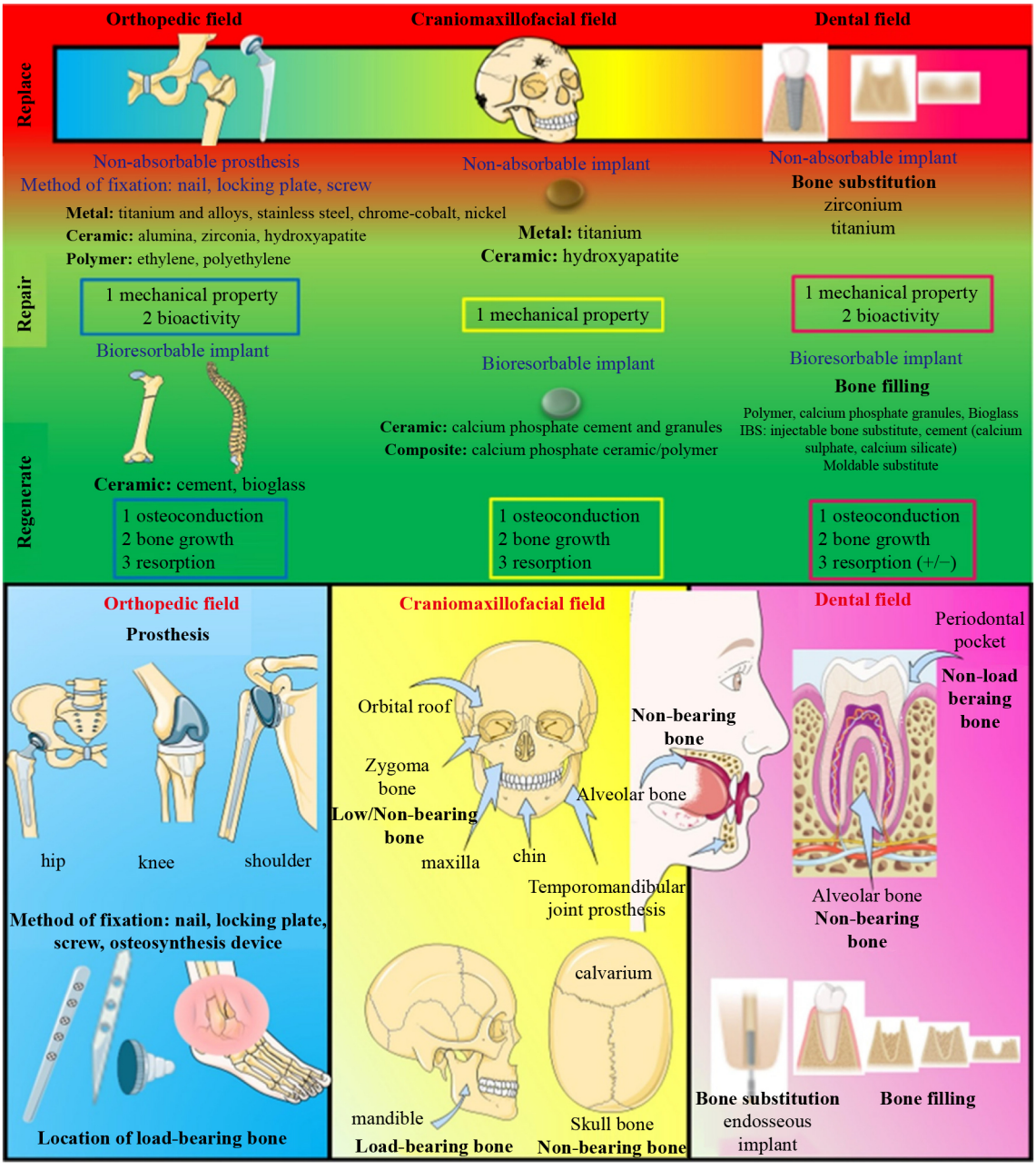

Fig. 9 Main approaches and different biomaterials used for treatment of bone tissue defects. Reproduced with permission from Ref. [52] (Copyright 2022, Elsevier).

including the need for a second surgical site operation and the evident scarcity of bone supplies, which can cause pain and morbidity at the donor site. Alternately, an allograft utilizing donor bone from a conventional bone bank might partially alleviate the bone supply shortage; but, following sterilizing procedures, the bone will lose its biological components and lose some of its strength. In addition, there are still worries about disease transmission and the patient's immune response to the donor bone. So, each bone graft has unique restrictions, costs a lot, and needs to be handled carefully. Therefore, there is a rising need for artificial bone substitutes that are unrestricted by the scarcity, variability, and illness of real bone [64]. Additionally, a technique known as "bone tissue engineering" may be used to combine these alternatives with the patient's own cells or recombinant growth factors to hasten or enhance bone healing. A rising amount of research is being done on "bone tissue engineering" as it is considered as a very promising approach for bone repair and regeneration.

4.3 Bone tissue engineering

Bone tissue engineering offers promising, interesting, and adaptable approaches to promoting bone repair and regeneration (Fig. 10 [31,65]). Cells, growth factors, porous scaffolds, and biophysical signals make up the mainstays of tissue engineering methods. Each of these elements can be used independently or in combination. Injection or transfer of stem cells, such as mesenchymal stem cells, to the fracture site may be used as a cell therapy for "bone tissue engineering" to aid neighboring cells in the process of repairing the bone. To encourage native or transplanted cells and hasten bone regeneration, growth factors such as bone morphogenetic protein-2 (BMP-2) can be released into bone defects at physiological dosages. Engineering of bone tissue scaffolds are frequently made of ceramic or polymeric materials that offer a framework for bone repair and can house cells at the site of the defect. It is possible to design the mechanical, chemical, topographical, and degradative characteristics of scaffolds to promote cell adhesion, proliferation, and differentiation or to administer regulated growth factors [66].

A porous scaffold, appropriate cells, and signaling biomolecules (e.g., growth factors and proteins) are the three main components of bone tissue engineering. Cells can attach to a scaffold surface, differentiate, and form new bone tissue in a biochemically relevant conditions involving growth factors. Bioactive materials that may react with bodily fluids to build bonds to native bone are used to create bone scaffolds that are intended to mend bone deformities. The regeneration of new vascularized bone tissue should be aided by the use of an appropriate bioactive porous scaffold together with pertinent cells and signaling molecules. High porosity and pore interconnectivity are necessary for bone scaffolds in order to promote bone cell adhesion and proliferation, in-growth of new bone tissue, and vascularization. It is important to emphasize that the porosity, pore size, and shape are crucial for good scaffold architectures. Fast cell attachment and development as well as significant nutrition and waste transfer rates are made possible by 3D porous scaffolds [66]. These structures also offer a substantial surface area for bone development. In order to achieve these goals, extremely porous scaffolds in 3D shapes are essential. Scaffolds should have a porosity of around 90%.

The selection of suitable biomaterials with acceptable mechanical characteristics is the first and most important prerequisite. The creation of scaffolds with appropriate structures is the next prerequisite. Different sorts of shapes and designs have been employed in bone tissue engineering to create medical implants and other devices. The mechanical characteristics of scaffold constructions are significantly influenced by their right design. Taken together, biocompatibility (not toxic to cells and tissues), biodegradability (relevant rate of biodegradation), bioactivity (can bond to tissue), relevant architecture (mimic ECM), and mechanical strength are all desirable qualities in biomaterials as summarized in Table 4 [12].

Collectively, higher spatial resolutions and hierarchical structural capabilities in scaffold processing quickly advance the ability of modifying the mechanical and biological response of biomaterials. Additionally, significant improvements in scaffold fabrication methods, namely, 3D printing, have increased the feasibility of designing scaffolds with pre-customized and personalized properties, i.e., 3D printing of a patient-specific scaffold. Along with this, bone tissue engineering offers very promising methods for accelerating bone repair and regeneration, which might lead to better therapeutic results for patients with bone fractures and complex bone defects [66].

4.4 3D printing process for bone tissue engineering

3D printing technology possesses a significant potential in bone tissue engineering owing to the high spatial architecture control that 3D printing allows to anatomically match irregular and complex shaped bone defects. The majority of 3D printing processes construct structures by a layer additive process using CAD models. The 3D print head moves along the *X-Y-Z* plane according to instructions from the CAD to construct a 3D object in by a layer-by-layer additive deposition process.

With the use of 3D printing technology, complex, personalized anatomical and medicinal structures may be created as a patient-specific scaffold by converting pictures from X-ray imaging, magnetic resonance imaging (MRI), and computed tomography (CT) scans into digital 3D print files [21]. Figure 11 depicts a schematic illustration of a 3D printing procedure used for bone tissue regeneration [67–68]. The procedure entails scanning the bone defect and producing a surface tessellation language (STL) formatted CAD file of the desired product. The printer then slices the CAD model data to create a 3D printed porous scaffold after receiving the file.

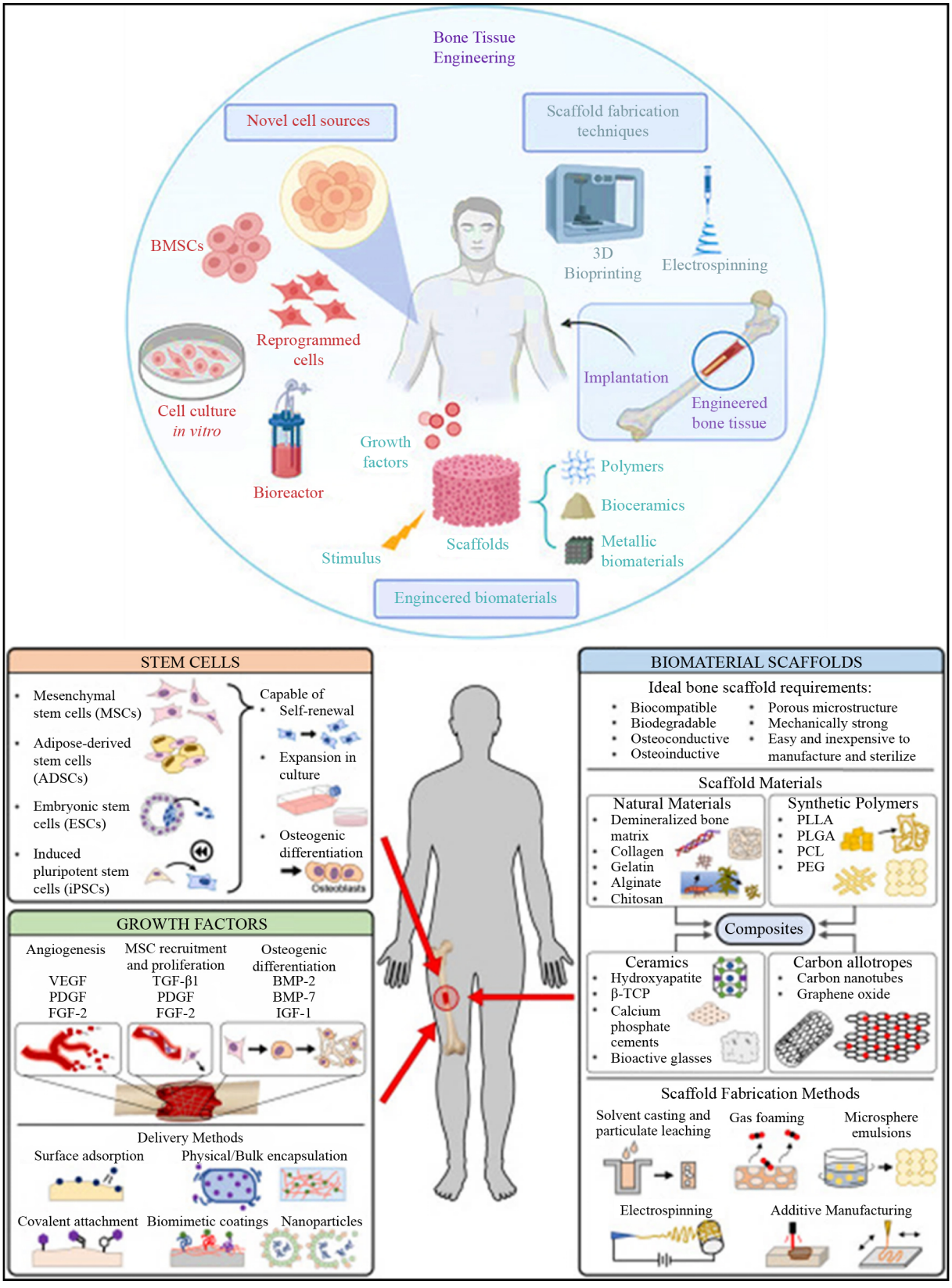

Fig. 10 Schematic illustration of bone tissue engineering approaches (upper panel) (reproduced with permission from Ref. [31], Copyright 2021, John Wiley and Sons). Examples of cells, growth factors, and biomaterial scaffolds used in bone tissue engineering (lower panel) (reproduced with permission from Ref. [65], Copyright 2022, Elsevier).

Table 4 General requirements for biomaterials scaffolds (reproduced with permission from Ref. [12], Copyright 2018, Elsevier)

Scaffold characteristic	Desirable features
Biocompatibility	• Non-toxic breakdown products • Non-inflammatory scaffold components, avoiding immune rejection
Biodegradability	• Controlled scaffold degradation which can complement tissue ingrowth whilst maintaining sufficient support • Degradable by host enzymatic or biological processes • Allows invading host cells to produce their own extracellular matrix
Bioactivity	• Scaffold materials that can interact with and bind to host tissue • Osteoconductive and osteoinductive properties • Inclusion of biological cues and growth factors to stimulate cell ingrowth, attachment and differentiation
Scaffold architecture	• Interconnected pores allowing diffusion and cell migration • Microporosity to present a large surface area for cell-scaffold interactions • Macroporosity to allow cell migration and invasion of vasculature • Pore size tailored to target tissue and cells • Sufficient porosity to facilitate cell ingrowth without weakening mechanical properties • Inbuilt vascular channels to enhance angiogenesis *in vivo*
Mechanical properties	• Compressive elastic and fatigue strength comparable to host tissue allowing cell mechano-regulation to occur and structural integrity to remain *in vivo* • Scaffold material that can be readily manipulated in the clinical environment to treat individual patient bone defects

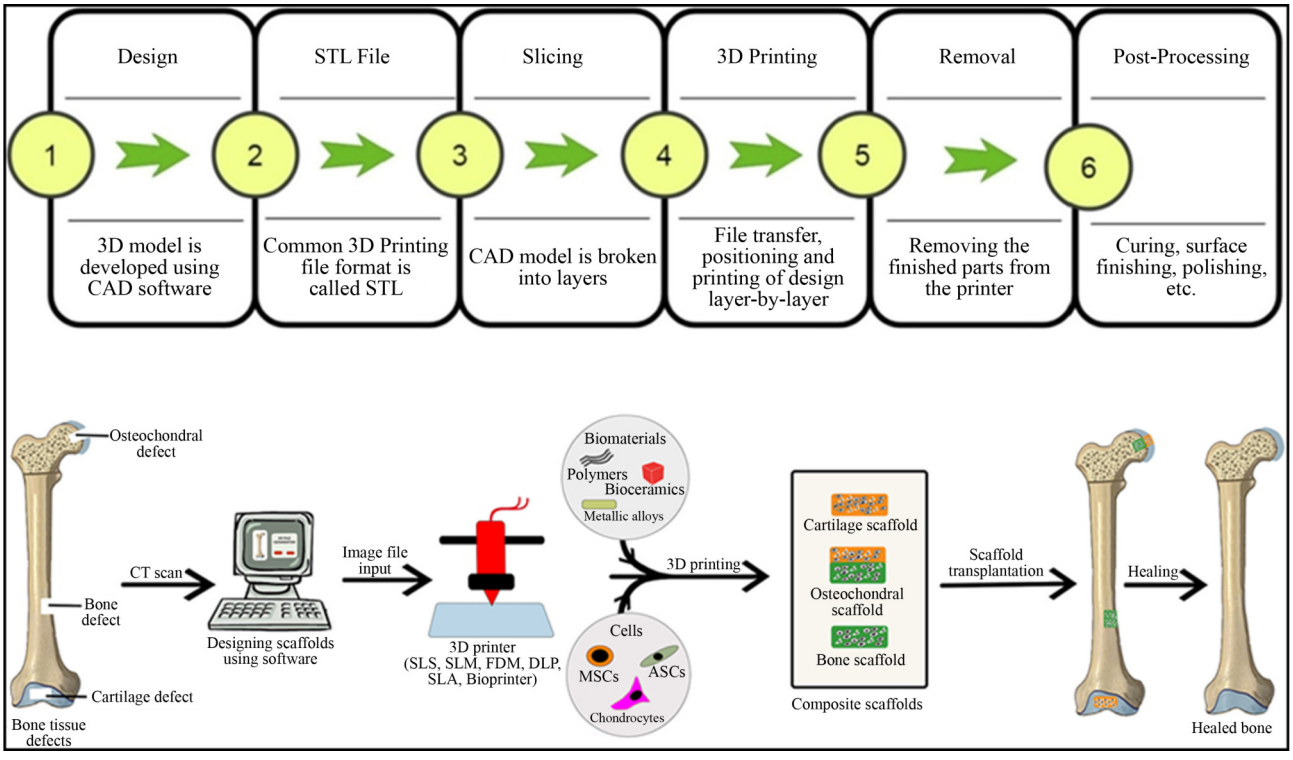

Fig. 11 Main steps involved in 3D printing process (upper panel) (reproduced with permission from Ref. [67], Copyright 2022, Elsevier). An illustrative example of 3D printing process for bone tissue engineering (lower panel) (reproduced with permission from Ref. [68], Copyright 2022, John Wiley and Sons).

4.5 3D printed biomaterials for bone tissue engineering

4.5.1 Biomaterials for scaffold fabrication for bone tissue engineering

Scaffolds for bone tissue engineering are manufactured using a variety of biomaterials, including natural and synthetic polymers, bioceramics, metals, and metallic alloys. Representative examples of common types of biomaterials that can be employed in scaffolds fabrication for bone tissue engineering are illustrated in Fig. 12 [69]. The most common biomaterials used for bone tissue engineering are bioceramics, e.g., hydroxyapatite (HA) and their composites with biopolymers. The biomaterials listed in Table 5 [12] does not necessarily have a wide variety of characteristics that meet every need for making scaffolds. As a result, composites — a term used to describe a mixture of two or more polymers, bioceramics, or metals — are employed to enhance the mechanical and biological performance of the scaffolds. By combining

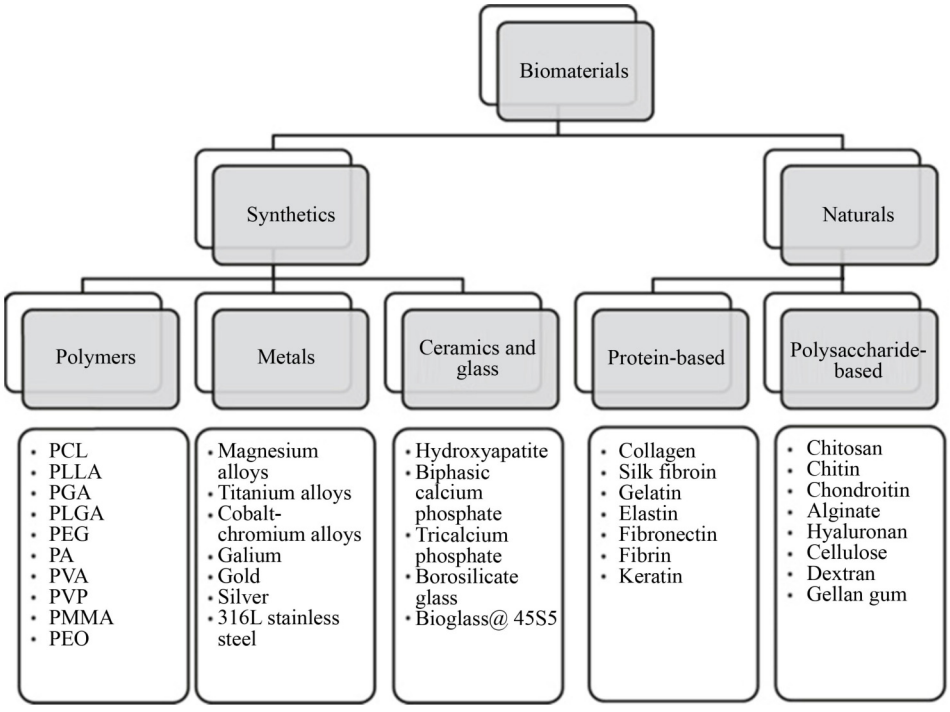

Fig. 12 Representative examples of common types of biomaterials used in scaffolds fabrication for bone tissue engineering. Reproduced with permission from Ref. [69]. Copyright 2019, Elsevier.

Table 5 Advantages and limitations of common types of biomaterials used in scaffolds fabrication for bone tissue engineering (reproduced with permission from Ref. [12], Copyright 2018, Elsevier)

Manufacturing material	Benefits	Potential limitations
Polymer	• Natural polymers can be derived from extracellular matrix, ensuring high biocompatibility and low toxicity • Biodegradable • Often contain biofunctional molecules on their surface • Synthetic polymers offer improved control over physical properties	• Natural and synthetic polymers generally lack mechanical properties for load bearing • Pathological impurities such as endotoxin that may be present in natural polymers • Synthetic polymers are often hydrophobic and lack cell recognition sites
Ceramic	• Osteoconductive and osteoinductive properties allow strong integration with host tissue • Similar composition to host bone mineral content • Can be delivered as granules, paste or in an injectable format	• Hard and brittle when used alone • May display inappropriate degradation/resorption rates, with decline in mechanical properties as a result
Bioactive glass	• Osteoconductive, osteoinductive properties • Adapted into clinical prosthesis already	• Inherent brittleness • Difficult to tune resorption rate • Manipulation of constructs into 3D shapes to treat specific defects is challenging • Potential for release of toxic metal ions
Metal	• Biocompatible • Superior strength • Superior mechanical properties can be advantageous in situations where slow bone growth likely	• Superior modulus can lead to stress-shielding • Poor biodegradability may result in further surgery/impairment of tissue ingrowth • Secondary release of metal ions may cause local and distal toxicity

two biomaterials, the unfavorable characteristics of one biomaterial are eliminated, making the scaffold more suitable for application. The advantages and drawbacks of biomaterials are also compared in Table 5.

4.5.2 3D printing techniques investigated for bone tissue engineering

Bone tissue is made up of two different components, namely cortical bone, which has less than 10% porosity, and cancellous bone, which has between 50% and 90% porosity. Porous scaffolds have been created using conventional techniques such freeze-drying, gas foaming, phase separation, salt leaching and electrospinning, but achieving the precise porosity levels that resemble native bones is very difficult using these conventional processing techniques. For example, it is difficult to get open pores when using the freeze-drying approach, however it is possible to construct a scaffold with more than 70% porosity. The gas foaming technique may be used to

create polymeric sponges with 90% porosity however, only 10% to 30% pore network interconnectivity can be attained. By using electrospinning, only 2D fibrous mats can be produced with a thickness less than 1 mm and consequently weak mechanical properties. Therefore, traditional processing approaches cannot manage the architecture and porosity of scaffolds to obtain certain features.

The issues with traditional processing methods can be avoided by 3D printing techniques. Although the scaffolds are created via a layer-by-layer process, 3D printing provide a number of advantages over traditional approaches, including the capacity to produce complicated shapes and provide well controlled porosity. More importantly, the ability to convert patient-specific bone deficiency images collected from CT/MRI scans to the required image format and deliver them as input to a 3D printer for creating patient-specific and customized bone scaffolds is a significant advantage of 3D printing techniques. For instance, better opportunities for enhancing the characteristics of bioceramics can be provided by 3D printing techniques. Actually, bioceramics used for bone tissue engineering need a certain porosity in addition to a customizable form to meet the bone defect geometry. Therefore, 3D printed porous bioceramic scaffolds come with many advantages over traditionally manufactured scaffolds. For example, 3D printed bioceramic scaffolds can be created with a tailored exterior form, intricate interior architecture, and carefully designed porosity. As a result, it is possible to make better control over key scaffold properties such as pore network interconnectivity, pore shape, and pore size.

Recently, various 3D printing techniques have been used to process bioceramics [70–78], bioactive glasses/mesoporous bioactive glasses [79–84], polymers [54,85–89], metals [90–93], and polymer/ceramic composites [19,56,94–109] into 3D printed porous scaffolds with a complex architecture and highly controlled porosity. For example, digital light projection and SLA based on UV-curable resin offer a good option to 3D print bioceramics with high geometric complexity [110]. Furthermore, for the creation of ceramics with large-scale dimensions and intricate porosity structures, digital light projection is a potential 3D printing method. Digital light projection is a form of light-based 3D printing. It uses a rotatable digital micron-sized mirror device to print scaffolds out of light one layer at a time. In order to create scaffolds, the light is directed onto a photosensitive polymer to induce photopolymerization. Digital light projection is a fast, precise 3D printing method that has produced encouraging results in several bone tissue engineering applications [111]. However, only photosensitive biomaterials can be printed with digital light projection. Indeed, the use of 3D printing techniques to create bone tissue 3D porous scaffolds is rapidly growing, and a variety of techniques are employed (Fig. 13). Percentages of different 3D printing techniques investigated for bone tissue engineering along with percentages of different tissue engineering applications using 3D printing techniques and a comparison of uses of different 3D printing techniques over time in bone tissue engineering are shown in Figs. 13(a)–13(c) [50].

4.5.3 3D printed porous scaffolds for bone tissue regeneration

Studies have demonstrated that 3D printed porous scaffolds can be used clinically to repair bone defects. For instance, a patient-specific 3D printed polycaprolactone (PCL) porous scaffold was used for the repair of significant and intricate maxillofacial deformities following the surgical resection of malignant bone tissue [112]. Furthermore, the effectiveness of the 3D printed porous scaffolds for bone tissue engineering has been demonstrated in several *in-vivo* animal studies [15,45,53,113–120]. Using the BJ-based 3D printing process, PCL/biphasic calcium phosphate (BCP) composite scaffolds with compressive strength and compression modulus equivalent to those of the human cancellous bone were reported by Ahn et al. [121]. Putra et al. [122] used extrusion-based 3D printing for producing iron-akermanite composite porous scaffolds with an open porosity of 69%–71%. The composites' *in-vitro* biodegradation rates were up to 2.6 times better than those of pure iron scaffolds that was geometrically equivalent. Even after 28 d of biodegradation, the scaffolds' yield strengths and elastic moduli were still within the range of the cancellous bone's mechanical characteristics. By using HA microspheres as an inorganic filler, Wei et al. [123] effectively printed a variety of HA/polylactic-co-glycolic acid (PLGA) 3D scaffolds with mechanical strength and chemical make-up comparable to natural bone. The highest compressive strength was recorded for the scaffold with 45% HA and it was six times higher than that of the neat PLGA scaffold. According to animal tests, the scaffold with 45% HA

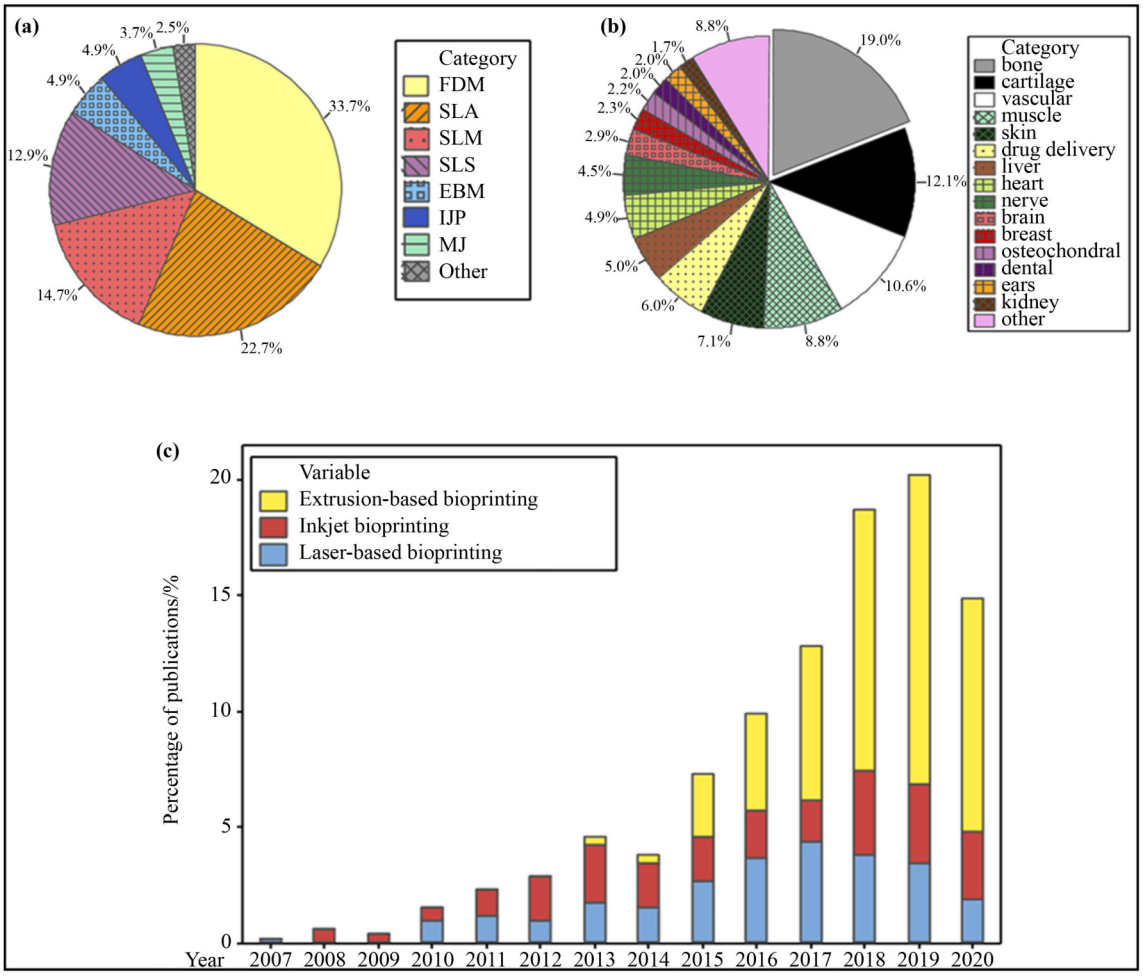

Fig. 13 (**a**) Percentages of different 3D printing techniques investigated for bone tissue engineering. (**b**) Percentages of different tissue engineering applications using 3D printing techniques. (**c**) Comparison of uses of different 3D printing techniques over time in bone tissue engineering. Reproduced with permission from Ref. [50] (Copyright 2020, Springer-Nature).

displayed the highest *in-vivo* stability and osteoinductivity. Figure 14 shows the stained histological sections of the PLGA, 30%HA/PLGA, and 45%HA/PLGA scaffolds after implantation into the rabbit femoral condyles for 4, 12, and 24 weeks [123]. The bone and cells are shown in red, violet, and blue, respectively, according to the results of the methylene blue and basic fuchsin staining. The 45%HA/PLGA scaffold's area shrank the most quickly after being implanted for 4 weeks (Fig. 14(d)). At the 4, 12, and 24 weeks, the new bone area of the 45%HA/PLGA scaffold was higher than that of the other two scaffold groups (Fig. 14(e)). At the area of the scaffold's edge where it has been implanted for 12 weeks, reasonably dense trabecular bone has developed, and good osseointegration has taken place with the feature of the almost complete absence of fibrous tissue at the bone-scaffold interface (Figs. 14(a′) and 15(a′)). Simultaneously, some bone-like tissue starts to accumulate in the scaffold's internal perforations (Fig. 15(d′)).

At the 24th week, fibrous tissue layers are seen at the interface between the new bone and the scaffold, while the bone mass in the inner pores of the PLGA scaffold does not considerably grow (Fig. 15(d″)). Overall, the two HA/PLGA scaffolds outperform the pure PLGA scaffold in terms of their ability to promote bone growth. There is evidence of new bone growth surrounding the three scaffolds. The maintenance of structural integrity, osteogenic activity, and osseointegration performance among the three scaffolds are noticeably different, despite of the similarity in degrading behavior.

Wang et al. [85] fabricated PCL/Zn composite scaffolds using FDM 3D printing to combine the benefits of PCL and Zn. They added zinc to PCL scaffolds with varying zinc powder levels (1, 2, and 3 wt.%).

The PCL/Zn composite scaffold showed better mechanical behavior and biocompatibility than the neat

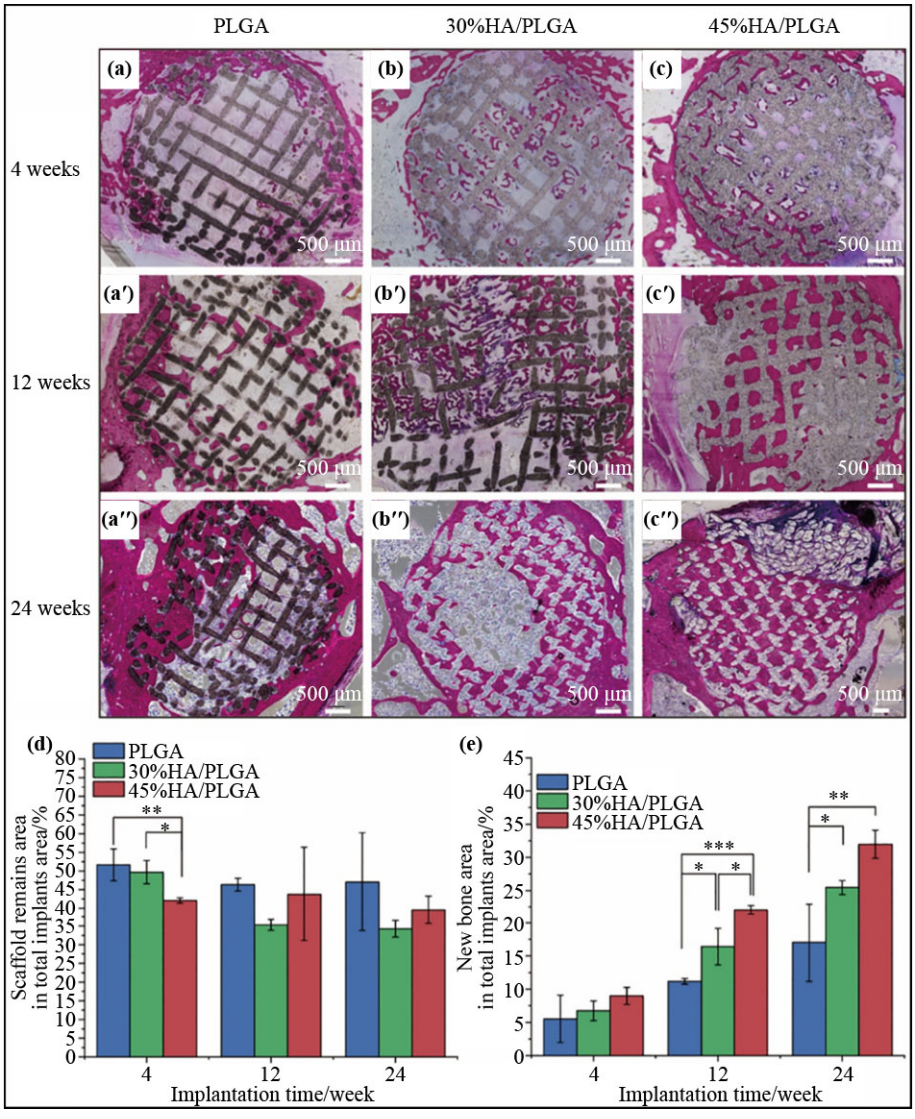

Fig. 14 Images of the stained histological sections of (**a**)(**a′**)(**a″**) PLGA, (**b**)(**b′**)(**b″**) 30%HA/PLGA, and (**c**)(**c′**)(**c″**) 45%HA/PLGA scaffolds, along with quantitative analyses of (**d**) the scaffold remains area and (**e**) the new bone area of the three scaffolds after implantation for 4, 12, and 24 weeks. Reproduced with permission from Ref. [123] (Copyright 2022, Elsevier).

PCL scaffolds. The addition of Zn powder increased the formation of new bone in a dose-dependent manner after 8 weeks following *in-vivo* implantation. The maximum osteogenic impact was seen in the scaffold with 2 wt.% Zn which make this scaffold ideal for bone tissue engineering. Mg-1Ca/PCL composite scaffolds were created by Zhao et al. [124] with 5, 10, and 20 wt.% of Mg-1Ca. Fused deposition modelling 3D printing technique was utilized to create porous scaffolds with precise macro- and microstructure. The biocompatibility of 5 and 10 wt.% composites was good. Additionally, these composites stimulated bone regeneration, according to microcomputed tomography and histological examinations. Therefore, it is anticipated that Mg-1Ca/PCL composite 3D printed scaffold may be a promising bone regeneration biomaterial for clinical use.

Scaffolds should imitate the characteristics of a mechanical support, biological activity, and extracellular matrix of native tissues. Additionally, scaffold acts as a guide for cell adhesion, proliferation, and promotes the formation of new bone tissue *in vivo*. Especially, the mechanical performance represents an essential property to success of scaffold in bone tissue engineering. Jakus et al. [113] utilized liquid extruded biomaterial inks at ambient temperature to make hyperelastic bone (HB), a new synthetic osteoregenerative biomaterial with 50% porosity. HB, which contains 10% PLGA and 90% HA, can be swiftly printed in three dimensions at rates of up to

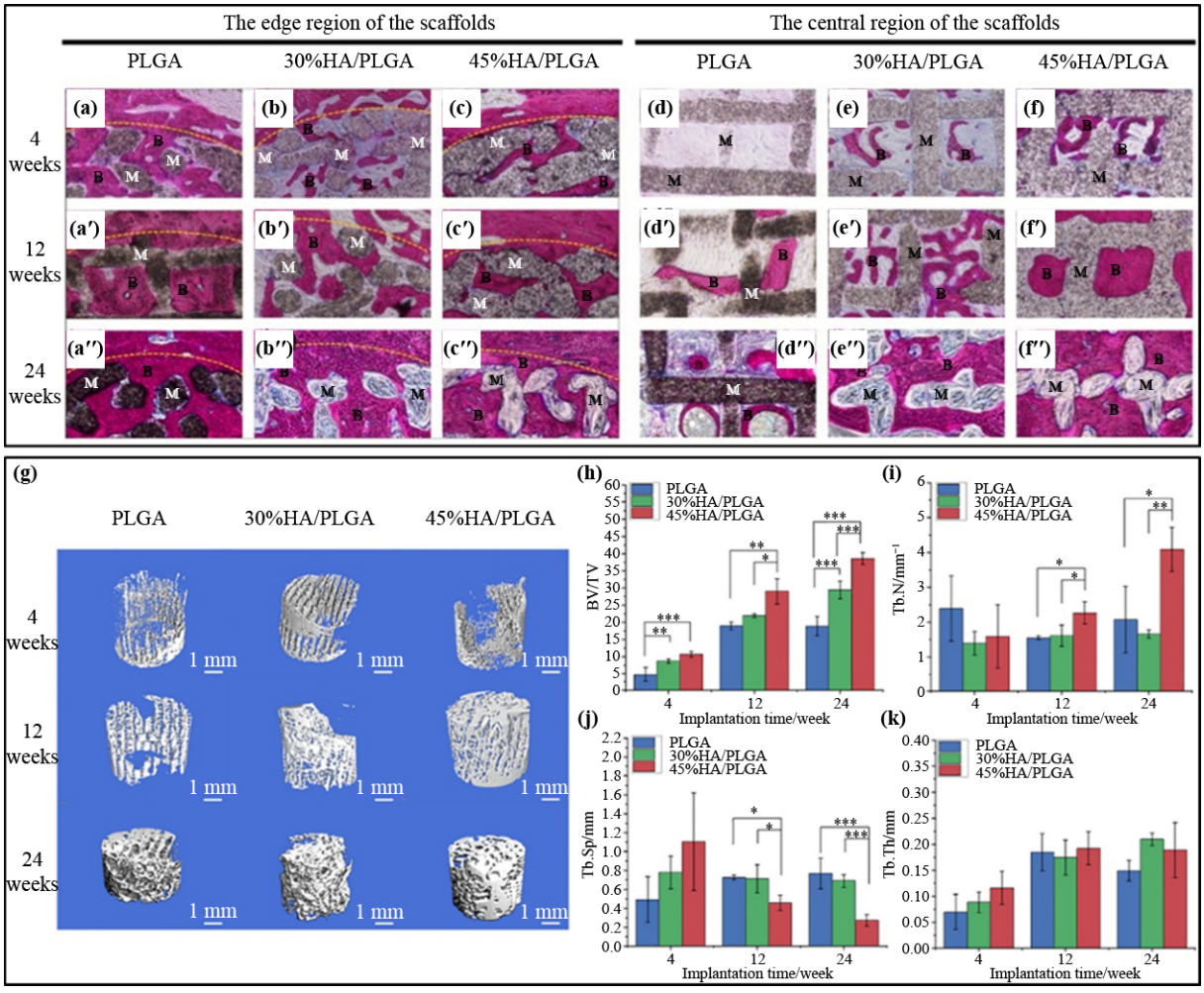

Fig. 15 (**a**)(**a′**)(**a″**)–(**f**)(**f′**)(**f″**) Magnified images of the edge and central regions of the scaffolds. M represents the scaffold material; B represents the new bone tissue; and the yellow dotted circles indicate the initial defect boundaries. 3D micro-CT reconstructed images of (**g**) new bone tissue, (**h**) quantitative analysis of the bone volume/total volume (BV/TV), (**i**) trabecular number (Tb.N), (**j**) trabecular separation (Tb.Sp), and (**k**) trabecular thickness (Tb.Th) of the three scaffolds after implantation for 4, 12, and 24 weeks. Reproduced with permission from Ref. [123] (Copyright 2022, Elsevier).

275 $cm^3 \cdot h^{-1}$. HB shows versatility, scalability, and manipulation of hyperelastic 3D printed bone scaffold. HB biomaterial inks were rapidly 3D printed into patient-specific grafts that were scaled in accordance with anatomy, such an adult human jaw.

Furthermore, extremely complex designs that would have been challenging to manufacture as a single monolithic product were combined using discrete 3D printed elements. Also, the ability to 3D print HB inks in normal environment without the requirement for post-sintering permitted the involvement of biomolecules which may improve tissue regeneration. Furthermore, HB exhibited highly elastic mechanical behavior with 32%–67% strain to failure and 4 to 11 MPa elastic modulus.

The 3D printed HB promoted cell viability, proliferation, and induced osteogenic differentiation in human mesenchymal stem cells (hMSCs) derived from bone marrow cultured *in vitro* over 4 weeks without the presence of any osteo-inducing factors in the medium.

The 3D printed HB scaffolds encouraged osteogenic differentiation while also supporting hMSC adhesion and proliferation. A mouse subcutaneous implant model for material biocompatibility was performed for 7 and 35 d along with a large non-human primate calvarial lesion case study was used to investigate HB *in vivo* in an animal model for 4 weeks. The HB scaffolds showed well integration with the host tissue *in vivo*. According to scanning electron microscope images of explanted scaffold tissues, the tissue had made good bonding with

the HB implant. HB rapidly ossified, vascularized, quickly integrated with surrounding tissues, did not cause a negative immunological reaction, and promoted the formation of new bone without the need for other biological components.

The FDM technique is easy and cheap, but the biomaterial, mostly a thermoplastic polymer-based biomaterial must be formulated into a filament for 3D printability. Furthermore, it is affordable, simple to use (post-processing is not essential), safe (no use of organic solvents), and fast technique. Recently, FDM has become a well-stablished 3D printing technique for fabricating 3D porous scaffolds for bone tissue engineering. Using FDM 3D printing technique, Wang et al. [96] effectively manufactured PCL/bioactive glass composites with varied ratios of bioactive glass (5, 10, and 20 wt.%). Scaffolds containing bioactive glass demonstrated greater compressive strength and hydrophilicity as compared to pure PCL scaffolds. The scaffold's increased hydrophilicity further improved the capacity for cell attachment and cell proliferation. Additionally, *in-vivo* tests on animal model showed that the PCL/bioactive glass scaffold with 20 wt.% of bioactive glass promoted bone regeneration more effectively than the pure PCL scaffold. The repair of complicated 3D bone defects in the craniomaxillofacial area is constrained by the sue of traditional grafts which are only applied in the form of block or powder forms. Additionally, due to the complicated structure of the craniomaxillofacial bones, scaffolds utilized for repairing bone loss in the craniomaxillofacial region should have special characteristics such as pre-customized architecture and patient-specific shape.

Customized kagome-structure scaffold with intricate morphology was developed by Lee et al. [114]. The 3D kagome-structure model was specially created for the defect site utilizing data from 3D computed tomography. A 3D printer equipped with a precision extruding deposition head and PCL was used to create the kagome-structure scaffold. A traditional grid-structured PCL scaffold was used as a comparison group. The two different kinds of 3D printed scaffolds were inserted into the rabbit calvarium's 8-shaped defect model (Fig. 16). In terms of mechanical strength, the kagome-structure scaffold was superior than the standard grid-structured scaffold. Additionally, the kagome-structure scaffold was made exactly to match the intricate bone defect, and it demonstrated superior osteoconductivity and great fitting ability with the defect margin. As a result, complicated craniomaxillofacial bone defects can benefit from the use of the kagome-structure scaffold for both aesthetic and functional repair. Figures 16(a)–16(d) depict the creation of an 8-shaped defect model on a rabbit calvarial (Fig. 16(a)), a computed tomography imaging (Fig. 16(b)), the design of a scaffold with a kagome structure (Fig. 16(c)), that is specifically tailored to the defect, and 3D printing using a PED head (Fig. 16(d)).

Figures 16(e)–16(h) show scanning electron microscopy (SEM) images of PCL scaffolds fabricated for 8-shaped defect model along with their optical images after implanted animal defect sites, whereas Figs. 16(i)–16(k) show the *in-vivo* performance of the implanted scaffolds. Collectively, the scaffold was made exactly to match the intricate bone defect in craniomaxillofacial region, and it demonstrated good bone forming behavior and great match with the defect shape. As a result, irregular bone defects in craniomaxillofacial region can benefit from the use of the customizable scaffold.

Making a scaffold from bioactive glass (a well-known bioactive biomaterial with excellent osteoinductivity, i.e., formation of new bone *in vivo*) with strong mechanical properties while maintaining unaltered properties remains a difficult task. Pure bioactive glass is not a printable material since it is a solid material and it lacks fluidity. The 3D printing methods currently being used to fabricate bioactive glass scaffolds either includes adding bioactive glass to a printable polymeric material along with subsequent sintering process to create pure bioactive glass scaffold [50] or combining bioactive glass with a printable biopolymer and forming bioactive glass/biopolymer composite scaffold [81].

Wang et al. [125] recently described a fabrication method combining self-assembly and 3D printing (SAP), and they successfully printed mesoporous bioactive glass (MBG) sol directly into a hierarchical SAP-MBG porous scaffold with a compact and integrated structure. The mechanical strength of the SAP-MBG scaffold was dramatically increased while maintaining the non-composite component and mesoporous structure. In a critical-size rat cranial lesion model, SAP-MBG demonstrated better porous network connectivity and quicker calcium dissolution, which improved cell in-growth, and *in-vivo* bone regenerating effectiveness. The SAP fabricating route was a viable strategy to get beyond the limitations of traditional production processes and enabled custom MBG scaffold manufacture. Distler and colleagues [55] demonstrated the successful fabrication of

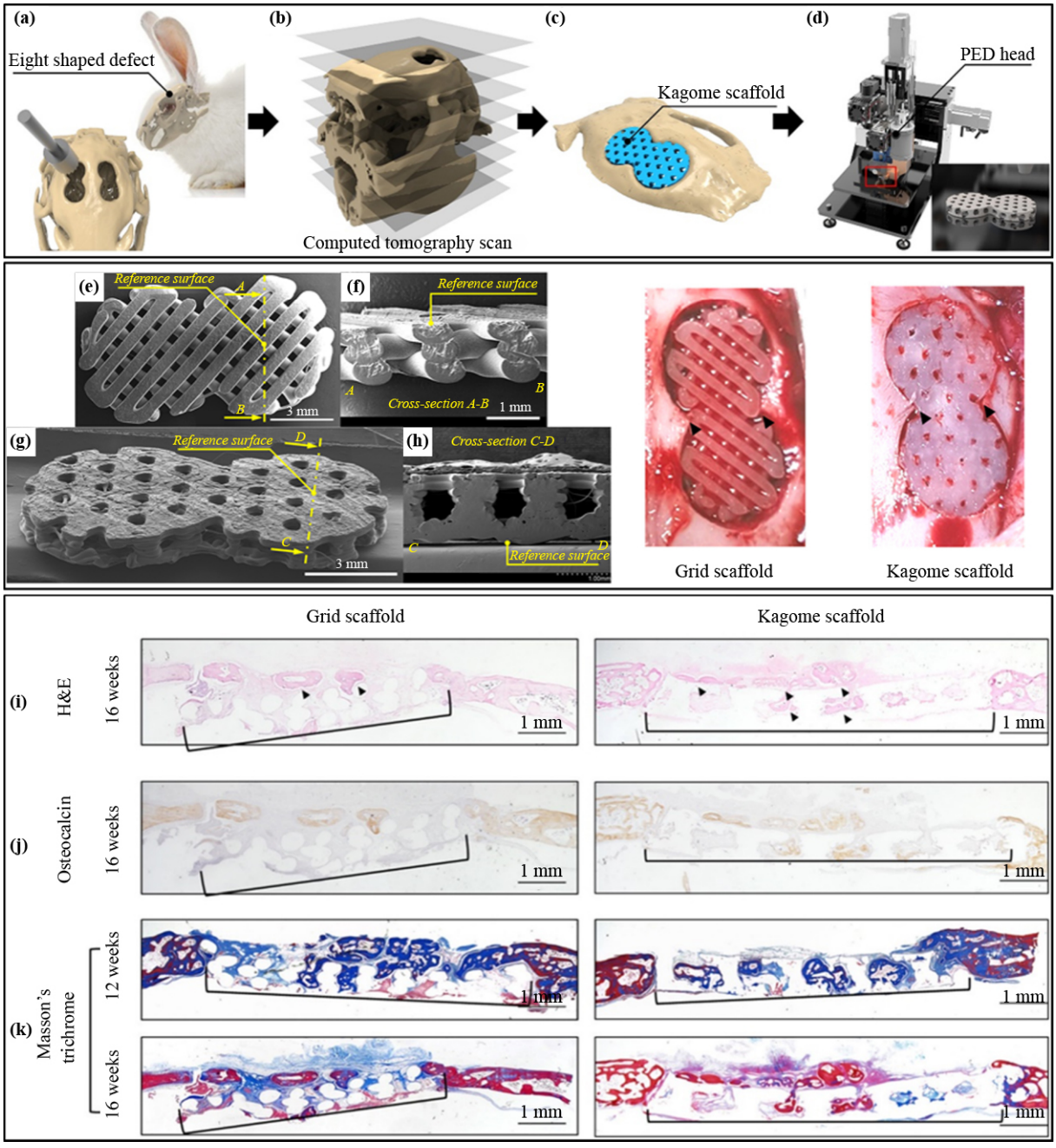

Fig. 16 (**a**) Making of the defect, (**b**) CT imaging, (**c**) design of customized scaffold, and (**d**) 3D printing. (**e**)(**f**)(**g**)(**h**) SEM images along with photos of *in-vivo* implanted scaffolds. Histology results of *in-vivo* study: (**i**) red color in lower panel, (**j**) orange color in lower panel, and (**k**) blue color indicating the new formed bone. Reproduced with permission from Ref. [114] (Copyright 2019, Elsevier).

polylactic acid/bioactive glass composite scaffolds using FDM 3D printing technique. Filaments of polylactic acid/bioactive glass were feasible to be prepared and to be 3D printed into porous scaffolds with a good precision. The successful printability of polylactic acid/bioactive glass filaments at high throughput without the use of solvents demonstrated that FDM is a promising 3D printing technique offering a flexible and possibly patient-specific biomaterial platform for bone tissue engineering.

Feng et al. [45] utilized FDM 3D printing to create polyetheretherketone (PEEK) scaffolds (upper panel in Fig. 17) with various pore diameters and medium porosities. The mechanical evaluation of PEEK scaffolds showed that the pore size had an impact on their mechanical performance. The increase in pore size

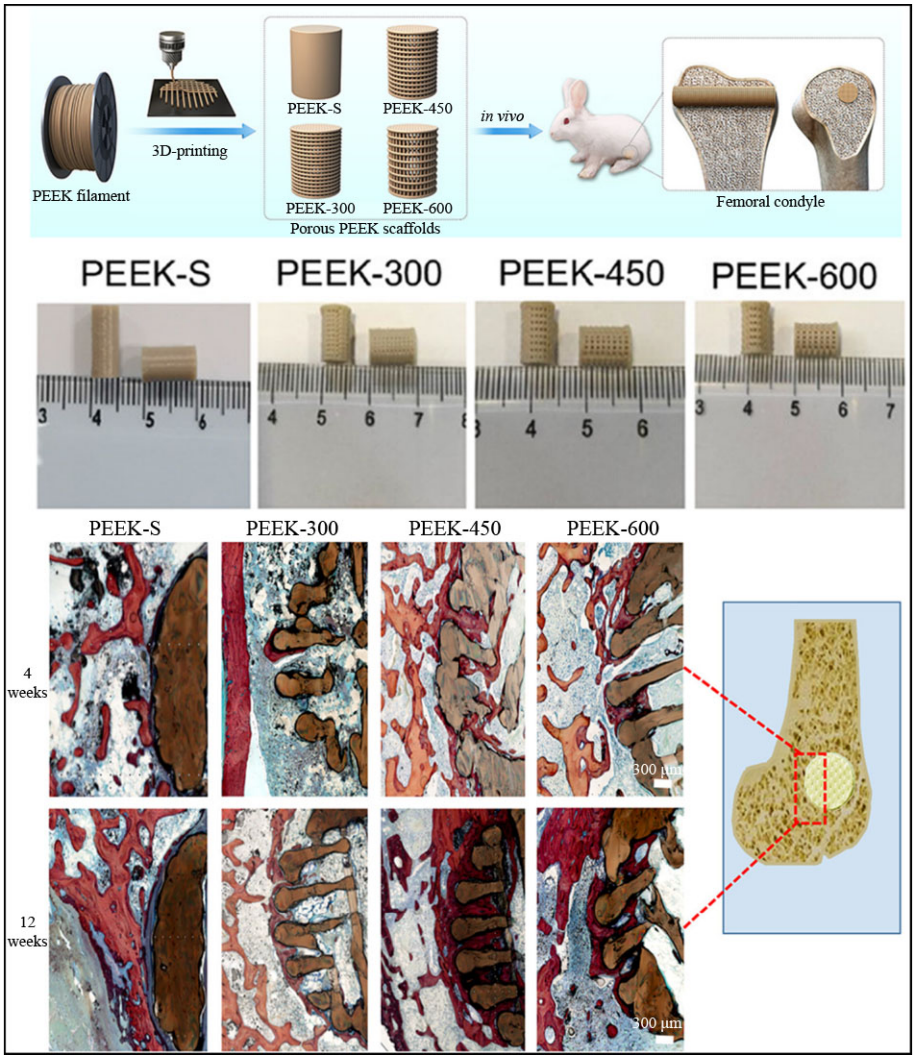

Fig. 17 Illustrative diagram of PEEK scaffolds fabricated by FDM process along with *in-vivo* animal model for implantation (upper panel). The *in-vivo* bone regeneration ability in animal model as revealed by histology (lower panel). Red color refers to newly formed bone tissues. Reproduced with permission from Ref. [45] (Copyright 2020, The American Chemical Society).

resulted in a considerable reduction in mean stiffness while the compressive stress and modulus nearly matched those of native trabecular bone. The PEEK scaffolds also showed a good cytobiocompatibility and promoted cell behavior in *in-vitro* stem cell cultures.

Furthermore, following the *in-vivo* implantation of PEEK scaffolds (solid PEEK samples named as PEEK-S were used as control scaffolds) for 4 and 12 weeks, histological investigation (lower panel in Fig. 17) of bone regeneration revealed new bone development (red color refers to newly formed bone tissues) around and inside the scaffolds as determined by hematoxylin and eosin staining. Also results showed direct connection between bone and the scaffold with newly generated bone tissues being developed into the pore region from the neighboring bone tissue. Especially, PEEK-450 scaffolds showed a preference for vascular perfusion and bone ingrowth.

Leftover malignant cells might cause a tumour growth following surgery for malignant cells bone fractures. Such tissue damage cannot be treated in a clinic with conventional implants. Consequently, it is vital to develop a new approach to provide implants with the dual functionality for tumour treatment and bone restoration at the same time. Wang et al. [126] developed calcium titanate ($CaTiO_3$) bioceramic scaffolds (CaTi) via 3D printing based on digital laser processing (DLP) technique for the treatment of tumour-induced bone disease. The DLP 3D printing has a good ability in managing the regularity in geometry and the precision of porosity of bioceramic scaffolds. CaTi scaffolds showed good

compressive strength and acceptable photo-thermal properties when subjected to laser. Moreover, under laser irradiation, the temperature of CaTi scaffolds exceeded 70 °C. CaTi scaffolds were employed for the treatment of bone tumor due to their superior photo-thermal performance. The CaTi scaffolds also have promising bone-forming properties both *in vitro* and *in vivo*. Therefore, CaTi bioceramic scaffolds created by 3D printing, namely DLP is a promising multifunctional biomaterial for treating tumour-induced bone defects. Wu et al. [115] reported 3D scaffolds with specified constant pore strut and tailorable pore height based on 6% Mg-substituted wollastonite (CSi-Mg6) powders using the SLA 3D printing technique. Figure 18 depicts the schematic stereolithographic method for creating bioceramic scaffolds with varying cell heights. The *in-vivo* performance of scaffolds in bone regeneration was revealed by micro-computed tomography (μCT) and histological analyses which showed that the ingrowth of newly formed bone tissue was slowed in H200 scaffolds

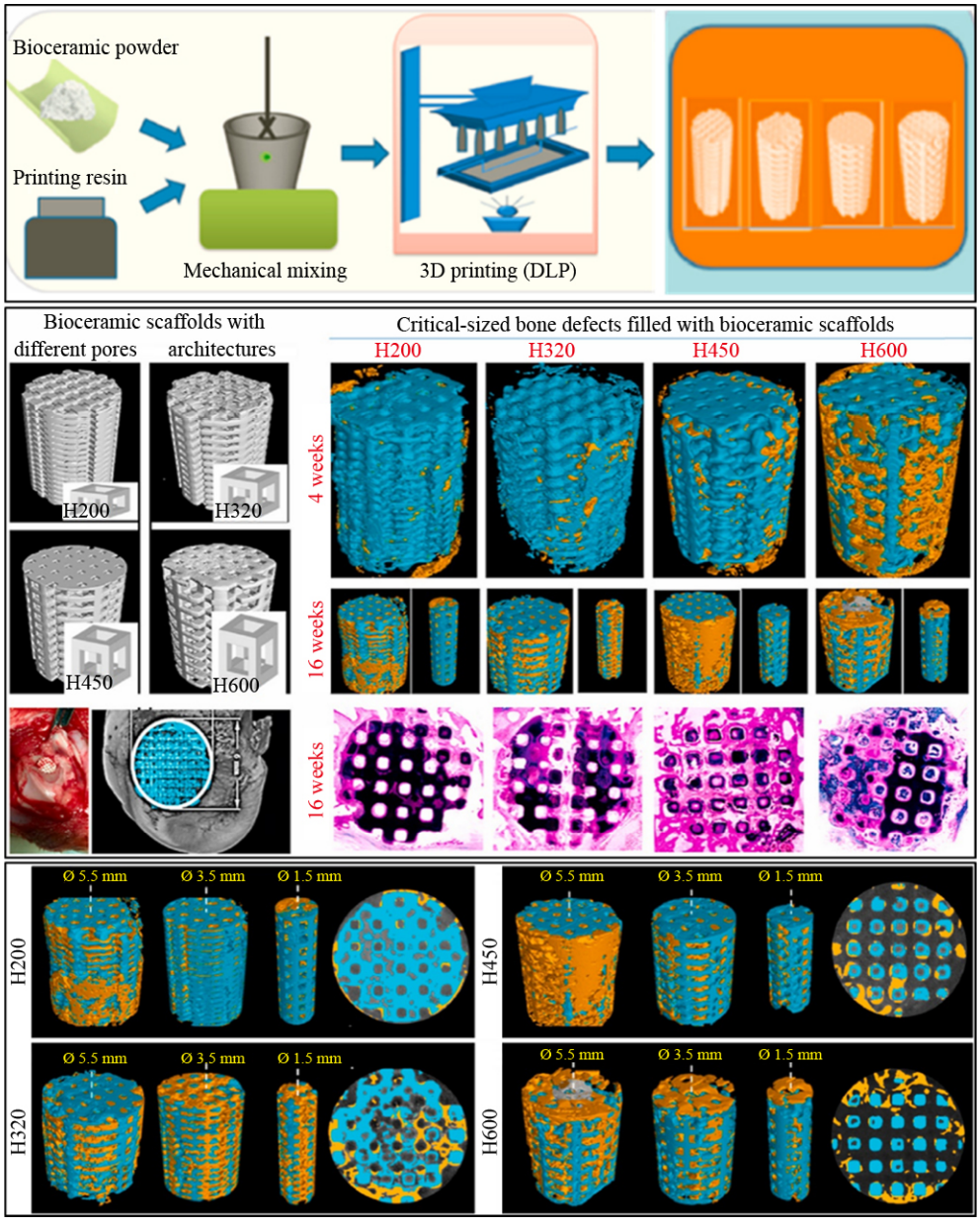

Fig. 18 Diagram of scaffolds preparation method (upper panel). CAD models and *in-vivo* study (middle and lower panels). Pink color in histology images refers to new formed bone. Yellow color in μCT reconstructed images (see the lower panel) refers to new formed bone. Reproduced with permission from Ref. [115] (Copyright 2021, Elsevier).

throughout the entire test stage, whereas the H320 scaffolds demonstrated considerable bone formation in the middle of the porous scaffolds and mature bone grown widely in the whole porous structure.

Notably, after two weeks, the bone ingrowth was facilitated in the H450 and H600 scaffolds, and at a later stage, there was a greater amount of bone regeneration and remodeling. The lower panel in Fig. 18 shows images of μCT reconstruction of scaffolds with new bone tissue as yellow color and scaffold biomaterial as blue color. In conclusion the study by Wu et al. [115] showed that 3D printed bioceramic scaffolds with precisely regulated pore structures have significant effects on the improvement of bone regeneration. By using the SLA 3D printing, Dong et al. [127] reported porous BCP bioceramic scaffolds with superior densification and mechanical characteristics. These bioceramic scaffolds exhibited isotropic dimensional reduction, in particular, mechanical features were comparable to those of native cortical bone. The BCP scaffolds showed medium porosity and good compressive strength. In addition to offering a new method for producing high-quality BCP bioceramic scaffolds with unique structure using the SLA 3D printing for bone tissue engineering, the study by Dong et al. [127] demonstrated the promising ability of SLA 3D printing to create BCP bioceramic scaffolds with desired properties. 3D printed β-tricalcium phosphate (β-TCP) and bone formation-inducing gene were coupled to create synthetic bone grafts as reported by Remy et al. [116]. Suspension-enclosing projection-SLA was used to create 3D printed β-TCP scaffolds that exhibited repeatable microarchitectures which improved the degradability and osteoconductive characteristics of β-TCP scaffolds. Figures 19(a) and 19(b) show a diagram of a 3D printer setup and the layer-by-layer construction method, respectively. Figures 19(c) and 19(d) show CAD files of 3D printed β-TCP scaffolds. Whereas, Figures 19(e) and 19(f) show μCT images of 3D printed β-TCP scaffolds. The *in-vitro* results showed that the gene transfection efficacy of both rat and human bone mesenchymal stem cells (hBMSCs) was improved by 3D printed β-TCP scaffolds coated with collagen incorporating bone formation-inducing gene. Additionally, hBMSCs osteogenic differentiation was improved. Furthermore, in critical-sized rat calvarial lesions, scaffolds with gene treatment greatly improved bone repair. Figure 19(g) shows histological analysis of new bone formation and integration of the implanted β-TCP scaffolds *in vivo*.

These study findings suggested that suspension-enclosing projection-SLA 3D-printed β-TCP scaffolds can be used to fabricate good scaffolds for bone tissue engineering. Martins et al. [128] outlined a precise printing method for customized HA constructions made by the DLP technology, which opened up a workable low-cost methodology to supply patient-specific bone transplant structures, specifically in the craniofacial region. It was possible to produce porous pieces from solutions containing up to 50% HA load with just 60% shrinkage. 3D printing made it feasible to produce tailored HA pieces according to the anatomical location by replicating porous and complicated bone architecture and even imitating the form of trabeculae, which is hard to do with conventional manufacturing processes.

For the precise design and construction of 3D printed scaffolds with intricate biomimetic structures, SLA can be employed with UV photopolymers. Zhang et al. [117] reported high mechanical strength 3D printed HA scaffolds manufactured using SLA and based on triply periodic minimum surfaces structures. Triply periodic minimum surfaces-structure based 3D printed HA scaffolds are shown in Figs. 20(a)–20(c). Figure 20(a) shows six triply periodic minimum surfaces models and HA scaffolds that were 3D manufactured using triply periodic minimum surfaces structures. Figures 20(b) and 20(c) show femur repair and skull patches which were created using structural biomimetic scaffolds based on the triply periodic minimum surface structure. Stress–strain curves for various constructions are shown in Fig. 20(d). The bionic bone scaffold's stress–strain curve is shown in Fig. 20(e). The range of cortical and trabecular bone's compressive strength is shown by the grey region. Scaffolding's compressive strengths with different constructions and apertures are displayed in Fig. 20(f). The Split-P structure's stress distributions and stress–strain curves when exposed to various aperture sizes are depicted in Fig. 20(g). The properties comparison of 3D printed triply periodic minimum surfaces-structured HA scaffolds with properties of other reported scaffolds are shown in Fig. 20(h). The *in-vivo* evaluation of Split-P and cross-hatch 3D printed HA scaffolds in femoral bone regeneration is shown in Fig. 21. A schematic of *in-vivo* femur implantation is shown in Fig. 21(a). The compression test of the scaffolds after 4, 8, and 12 weeks of implantation is shown in Fig. 21(b).

The 3D μCT images of new bone growth around the scaffolds after 4, 8, and 12 weeks of implantation is

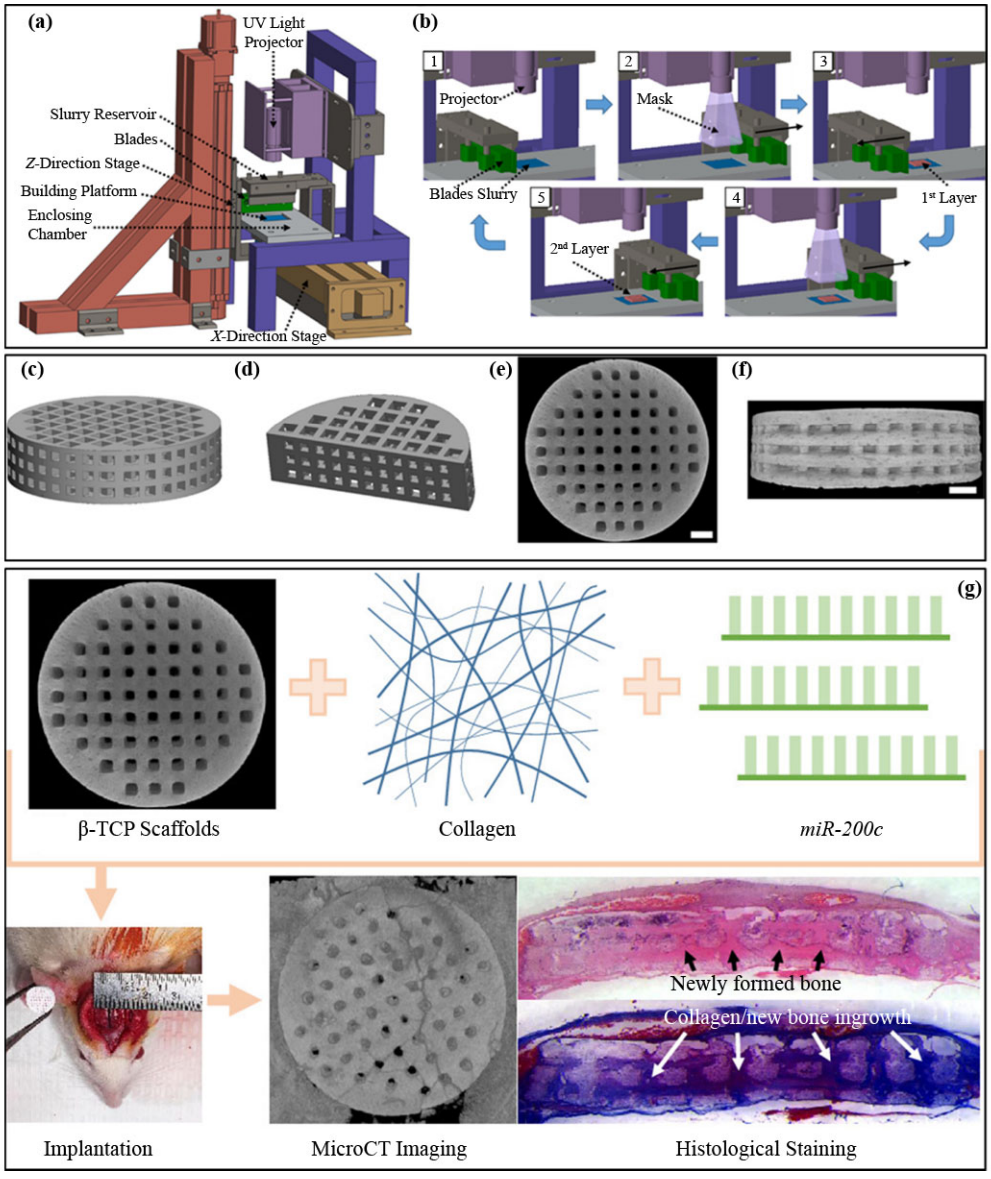

Fig. 19 (**a**)(**b**) Pictorial diagrams of scaffold fabrication process using suspension-enclosing projection-SLA 3D printing. (**c**)(**d**)(**e**)(**f**) CAD models and μCT images. (**g**) Scaffold combination and *in-vivo* study in an animal model. Reproduced with permission from Ref. [116] (Copyright 2021, The American Chemical Society).

shown in Fig. 21(c). Quantitative analysis of bone volume/total volume ratios (BV/TV), trabecular thicknesses (Tb.Th), and trabecular separations (Tb.Sp) of the scaffold samples at 4, 8, and 12 weeks after implantation is shown in Fig. 21(d). As the scaffolds were implanted into the rabbits' femoral medullary cavities, the scaffolds in the Split-P group had a noticeable increase in compressive stresses during early stages of the *in-vivo* implantation (Fig. 21(b)). In contrast to cross-hatch scaffolds, Split-P scaffolds exhibit much higher amounts of new bone formation (Fig. 21(d)) and enhanced osteoconductivity because new bone adheres to their surface and penetrates them through their pores (Fig. 21(c)). Thus, the findings of this study by Zhang et al. [117] demonstrated that triply periodic minimum surfaces-structured HA scaffolds outperform conventional HA scaffolds with cross-hatch structures in terms of compressive strength. These scaffolds also have a greater compressive strength range that is sufficient to meet the strength requirements for human cortical and trabecular bone.

Pant et al. [129] optimized the settings of extrusion-based 3D printing process for the production of MBG/PCL-based composite scaffold. The scaffold was tailored to have MBG to PCL ratio corresponding to 70:30

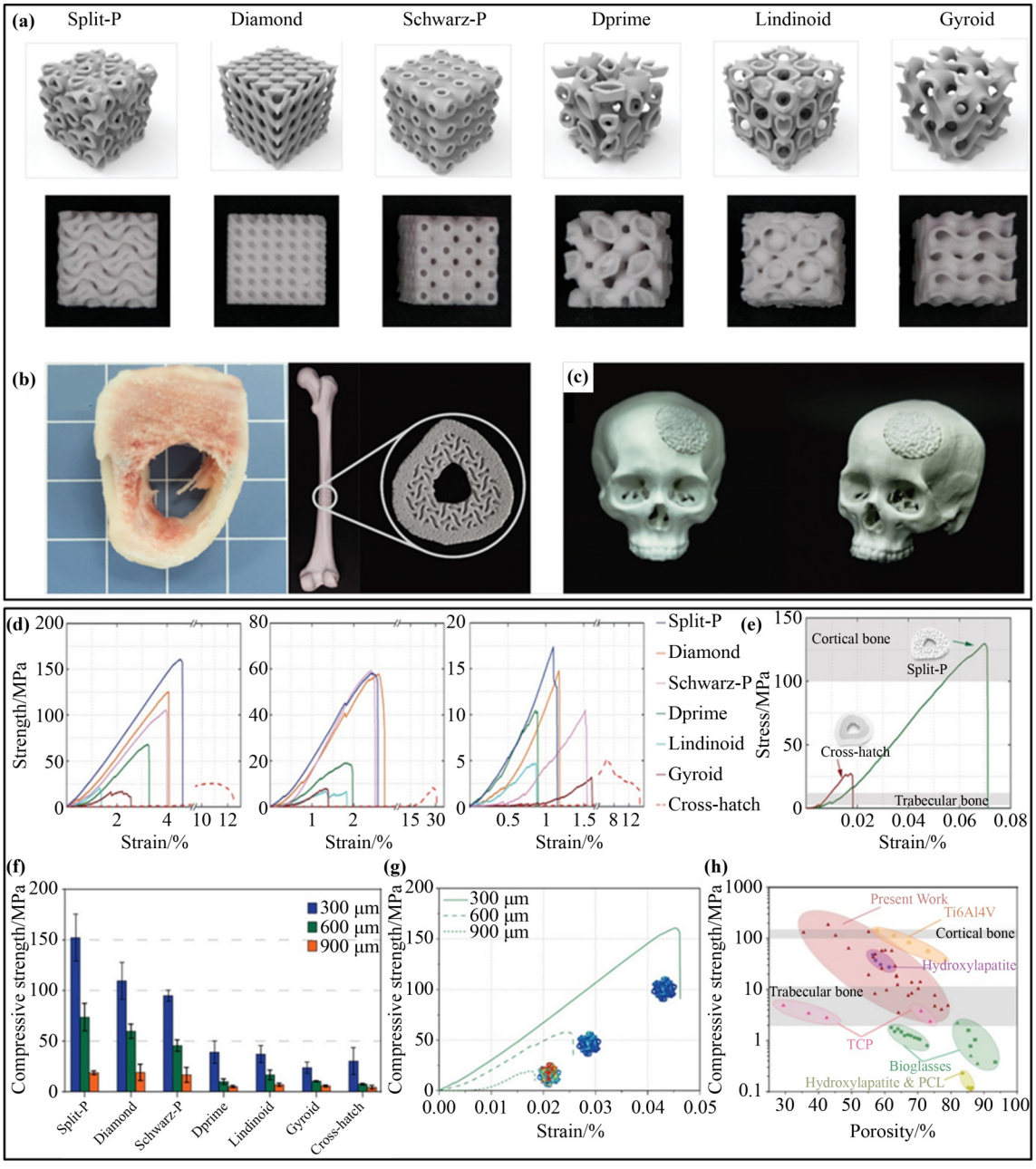

Fig. 20 (**a**) CAD models and images of 3D printed HA scaffolds. (**b**)(**c**) Specific 3D printed HA scaffolds for femur and skull bone defects. (**d**)(**e**)(**f**)(**g**)(**h**) Mechanical behavior of the 3D printed triply periodic minimum surfaces-structured HA scaffolds. Reproduced with permission from Ref. [117] (Copyright 2022, John Wiley and Sons).

mass ratio and a hierarchical pore structure to match the properties of natural bone. The ideal processing temperatures for creating pure PCL scaffold and MBG/PCL-based composite scaffold were 120 and 220 °C, respectively. The 3D printed PCL/MBG composite exhibited a 161% higher compressive elastic modulus than the pure PCL scaffold. Accordingly, the 3D printed MBG/PCL-based composite scaffold that mimics the features of natural bone can be considered as a promising scaffold for bone tissue engineering.

Using the SLS technique, bioactive glass scaffolds with different pore structures and different porosity levels were reported [130]. Scaffolds having porosities ranging from 60% to 30% had compressive strengths ranging from 1.7 to 15.5 MPa. However, after the scaffolds were submerged in simulated bodily fluids for a week, the scaffold's compressive strength drastically dropped (up to 90%). Overall, the findings of this study showed that the

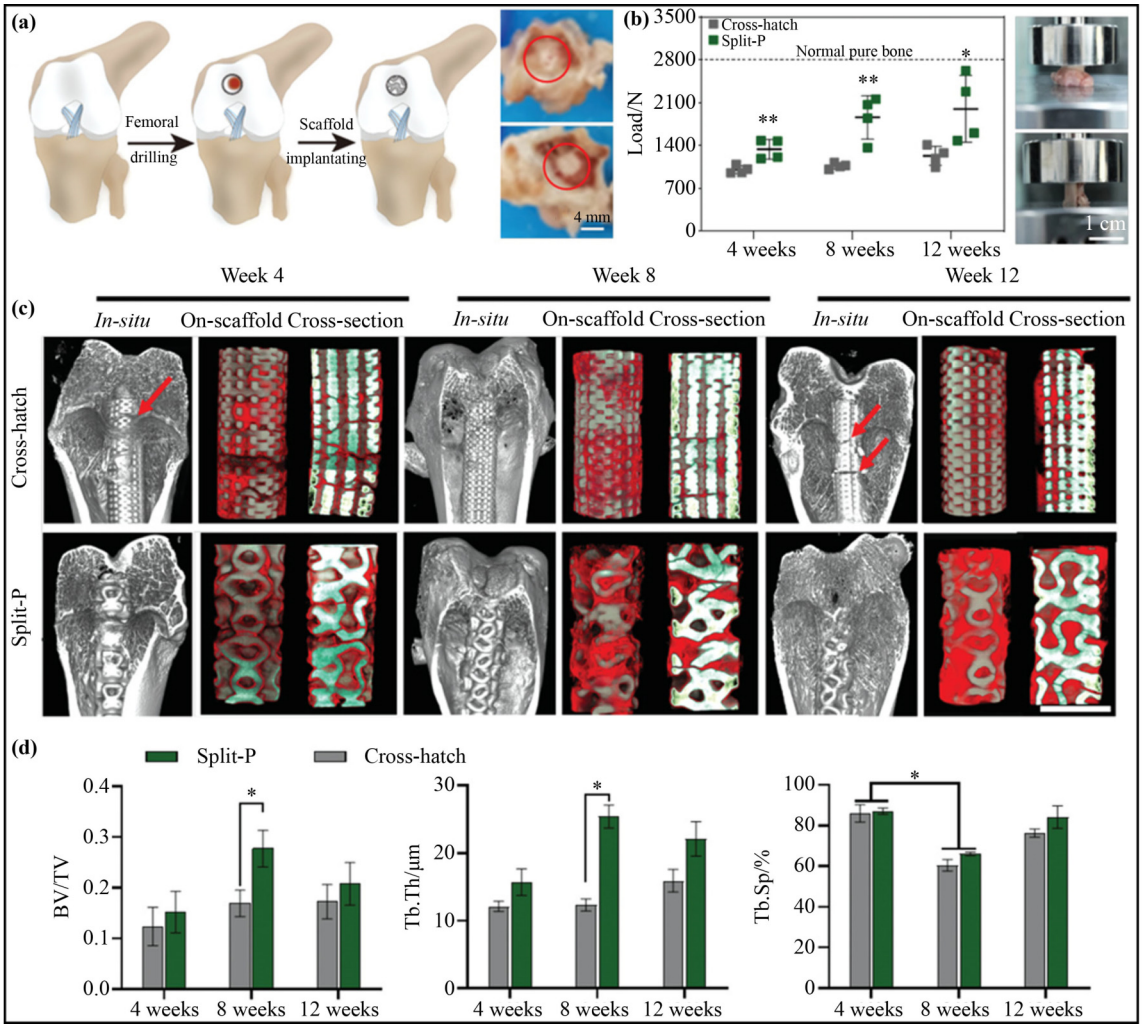

Fig. 21 (**a**) Schematic of *in-vivo* femur implantation, (**b**) the compression test, (**c**) μCT images, and (**d**) quantitative analysis of new bone formation of the scaffolds after 4, 8, and 12 weeks of implantation. The red color refers to the new bone tissue while the white color indicates the HA scaffold material. Reproduced with permission from Ref. [117] (Copyright 2022, John Wiley and Sons).

SLS technique can be used to fabricate borate bioactive glass scaffolds that might be used for bone tissue engineering.

Raymond et al. [118] demonstrated that printing calcium phosphate scaffolds with special architecture is feasible by changing the nozzle's shape during direct ink writing. The appearance of fabricated scaffolds is shown in Fig. 22 (upper panel). The efficacy of the fabricated calcium phosphate scaffolds was compared *in vivo* for their bone formation performance.

According to the *in-vivo* findings shown in Fig. 22 (left upper panel), the 3D-printed star-shaped scaffolds have greater osteoconductive qualities, directing newly generated bone more quickly into the scaffolds' core and promoting new bone regeneration. Thus, the study by Raymond et al. [118] reported a possible method to improve bone regeneration on 3D-printed scaffolds by controlling the shape of the scaffold filaments. Instead of the more conventional cylindrical filaments, star-shaped filaments seem to be able to guide bone into the center of the scaffolds more quickly.

Xu et al. [119] applied the DLP 3D printing technique in manufacturing of macroporous dome-like meshes based on wollastonite (CSi) 6% and magnesium doped wollastonite bioceramics (CSi-Mg6) at varied CSi/CSi-Mg6 mass ratios (0:100, 16:84, and 32:68). Figure 23 (upper panel) shows a schematic of the DLP 3D printing technique used to manufacture 3D wollastonite bioceramic scaffolds. According to the findings of this study, scaffolds containing 16% CSi had good mechanical qualities and encouraged osteogenic stem cells to proliferate and differentiate. Although the increase in

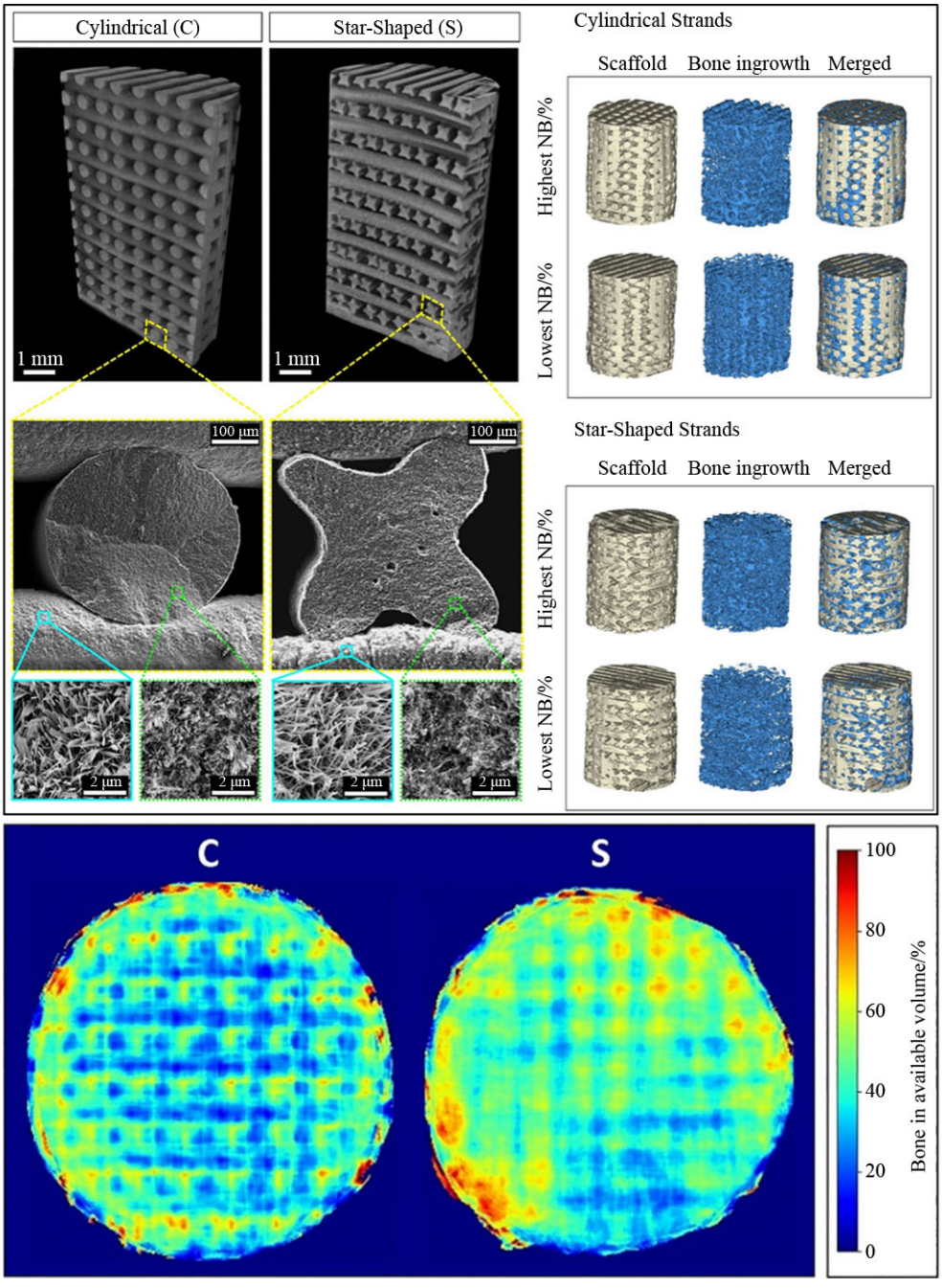

Fig. 22 Scaffold observations by μCT and SEM imaging (upper panel) along with cumulate mapping of the formed new bone (NB) (lower panel). Reproduced with permission from Ref. [118] (Copyright 2022, Elsevier).

wollastonite percentage is not favored for the mechanical strength and mechanical stability of the scaffolds, the CSi/CSi-Mg6 dome scaffolds demonstrated acceptable mechanical characteristics *in vitro*. In comparison to titanium mesh, the 16% CSi-containing bioceramic scaffolds demonstrated substantial biological activity by encouraging cell growth, increasing levels of bone-related genes, and the ingrowth of new bone. After 16 weeks of implantation, the dome scaffolds could sustain the porous structures particularly, the bioceramic dome's with 16% CSi significantly balance the scaffold's biodegradation and bone restoration. Actually, the 16% CSi dome scaffold were able to sustain stability for over 4 months *in vivo*. The results of *in-vivo* study are displayed in Fig. 23 (middle and lower panels). Reconstructed μCT images (in two- and three-dimensions) of the scaffolds after implantation are shown in Fig. 23 (middle panel) with yellow color referring to new bone while white color

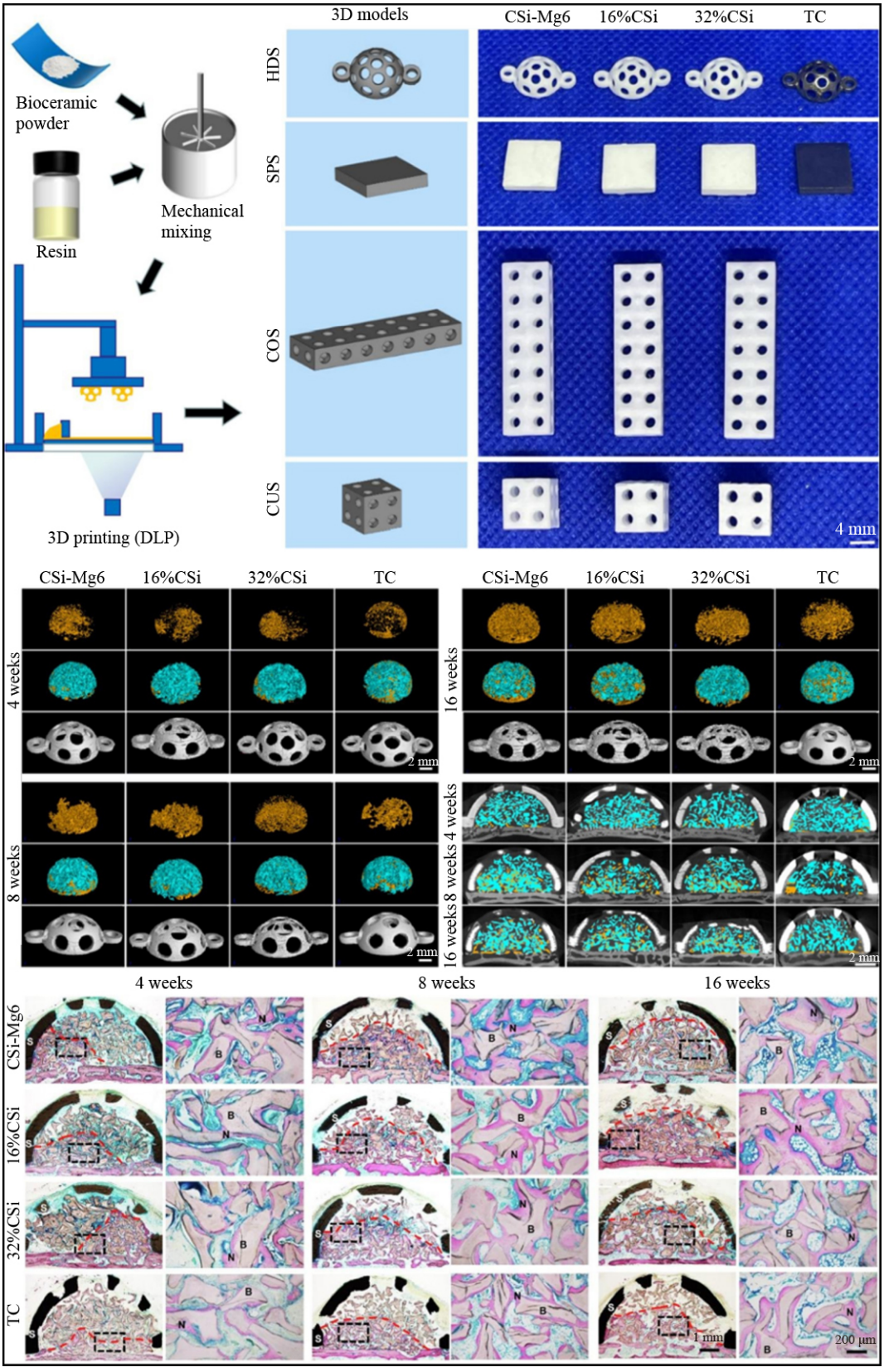

Fig. 23 Fabrication process (upper panel) and *in-vivo* study (middle and lower panels) of wollastonite bioceramic scaffolds. Reproduced with permission from Ref. [119] (Copyright 2022, Elsevier).

indicates to scaffolds. Typical histological sections of the samples at 4–16 weeks after surgery (methylene blue-acid magenta staining) are shown in Fig. 23 (lower panel). The scaffold is denoted by the symbol "S", the new bone by the symbol "N", and red lines refer to the growth height of new bone. In conclusion, DLP 3D printing was effectively used by Xu et al. [119] to create wollastonite bioceramic 3D printed scaffolds with high mechanical performance and good biological properties.

Using the digital light projection technology, Zhang et al. [120] produced a large-scale hydroxyapatite porous scaffold (length >150 mm). The DLP printing biomaterial ink mainly contained HA particles and photosensitive resin. Figures 24(a) and 24(b) show illustrative schematic of scan process of the implant digital model along with the DLP technique. Precision test of the DLP technique is

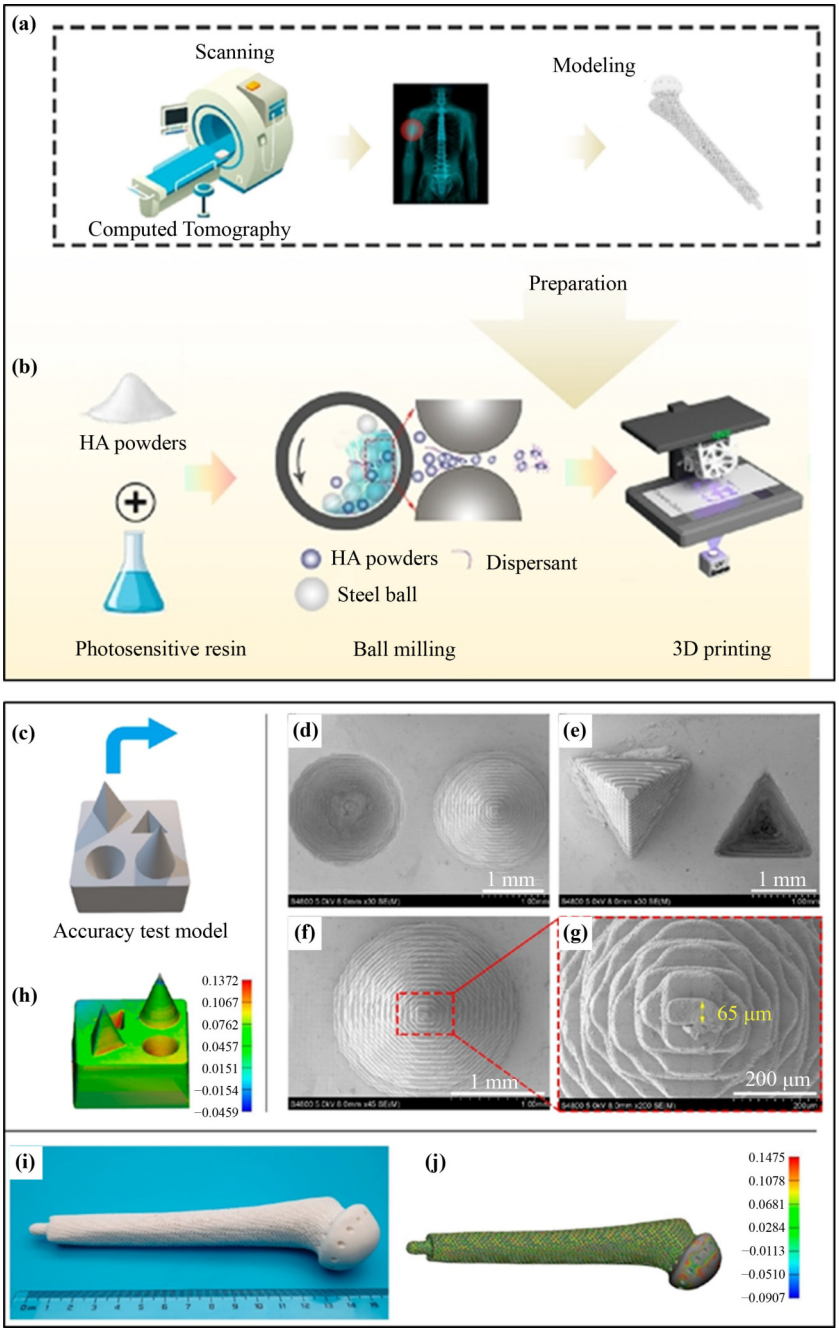

Fig. 24 Illustrative schematic of (**a**) the scan process and generating CAD model along with (**b**) the DLP technique. (**c**)–(**j**) Precision testing of DLP including SEM imaging. Reproduced with permission from Ref. [120] (Copyright 2022, The American Chemical Society).

shown in Figs. 24(c)–24(j). The precision test model is depicted in Fig. 24(c) along with the SEM imaging of the precision test object by the DLP technique in Figs. 24(d)–24(g). A comparison between the printed green body and the accuracy test model is also shown in Fig. 24(h). A full-size implant of a human humerus bone alongside the comparison between the printed green body and the humeral implant model is displayed in Fig. 24(i). With a printing precision of only 65 μm, the 3D printed scaffold featured extremely micro-nanoporous surface patterns that could be tailored by modifying the solid composition and sintering technique. The findings of this study suggested that DLP technology has the ability to manufacture precise porosity large-scale bone tissue engineering scaffolds. The developed 3D printed HA porous scaffold showed remarkable bone regeneration capabilities according to *in-vitro* and *in-vivo* studies. The scaffold was penetrated and integrated with the surrounding, as seen by μCT picture in Fig. 25 (upper panel). The fluorescence images revealed new bone development (middle panel in Fig. 25). The outstanding osteoinductive qualities of the DLP-printed scaffold were also demonstrated by the presence of bone tissue with a length of more than 500 μm in some of the pores. The

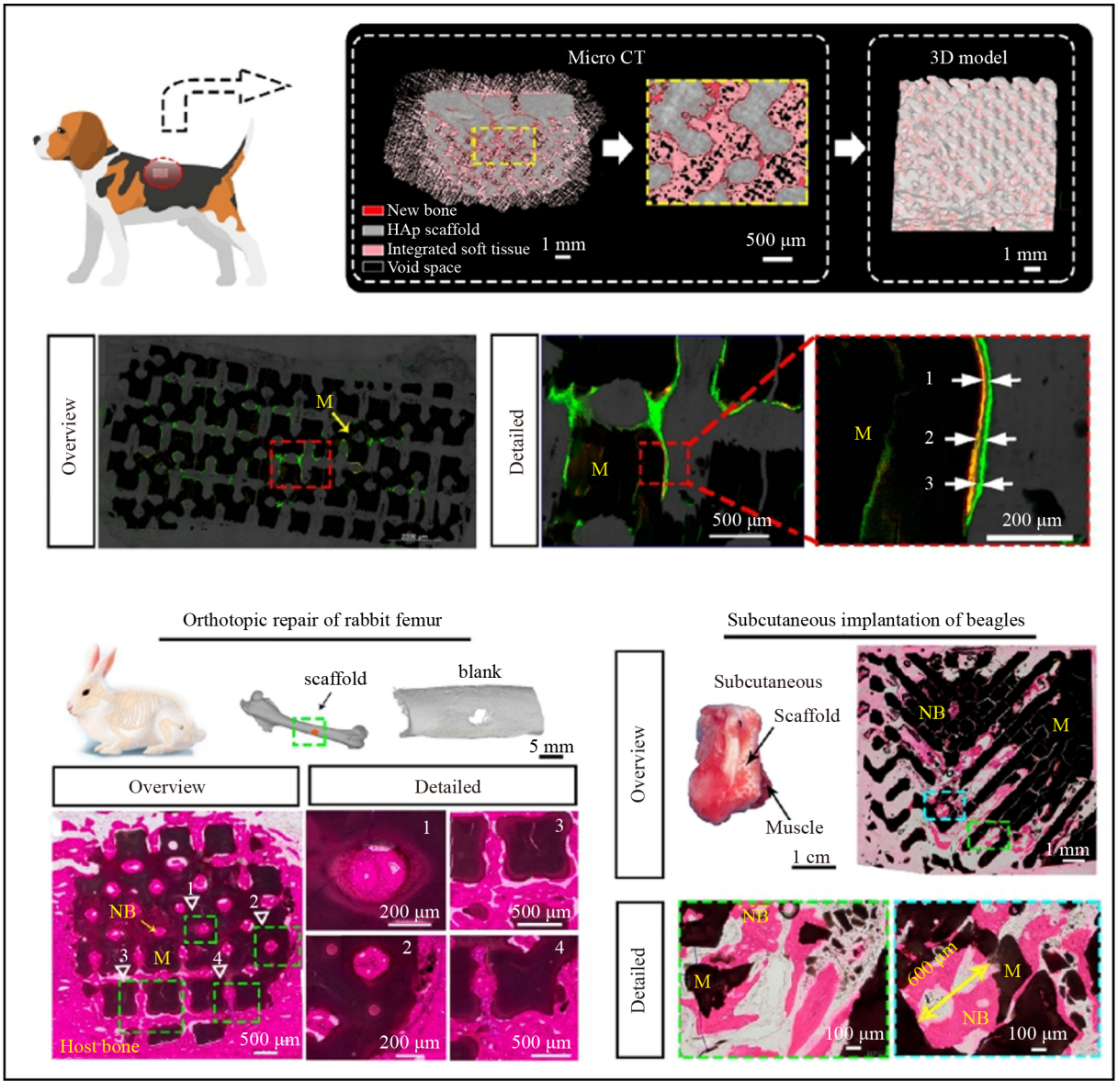

Fig. 25 *In-vivo* animal model and *in-vivo* analysis of new bone formation using μCT imaging, fluorescent staining and histology. NB denotes new bone. Reproduced with permission from Ref. [120] (Copyright 2022, The American Chemical Society).

in-vivo findings demonstrated that the scaffold is occupied by new bone (lower panel in Fig. 25). The study by Zhang et al. [120] showed that the DLP technique is a promising 3D printing platform for mass production of bone tissue engineering scaffolds in addition to a good feasibility for manufacturing of customized orthopaedic implants.

The feasibility of producing large (>1000 mm^3) 3D PCL/BG composite scaffolds with direct ink writing was recently reported by Baier et al. [81]. Despite being rather large (>1000 mm^3), the scaffolds were constructed with good resolution and high accuracy. A zig zag-spiral-patterned 3D printed polymeric scaffold was introduced by Fallah et al. [86]. The scaffolds had the same amount of porosity and permeability as native bone. The findings of the study by Fallah et al. [86] demonstrated that cells in scaffolds with a zig zag-spiral design gradually filled pores, whereas other scaffold forms required more time. Scaffolds with zig zag-spiral patterns can imitate the qualities of cancellous bones and be a promising option for treating bone defects. Shao et al. [75] developed a projection-based 3D printing (3DPP) machine appropriate for producing very accurate hydroxyapatite ceramic constructs. A paste with a solid composition of 50% made from micron HA powder and resin was prepared and used for 3DPP. The layer thickness, light intensity, and exposure duration were found to be the most effective printing parameters for the HA ceramic paste. The HA scaffold demonstrated high compressive strength and high compressive modulus. The *in-vitro* findings showed that the HA scaffold had no discernible cytotoxicity and that, because of its composition and design, cells adhered to it better and multiplied and differentiated more readily. According to the results of this study, 3DPP technology is also perfectly suited for creating ceramic structures with precisely regulated forms, which are highly needed for bone tissue engineering.

PEEK scaffolds are used in the dental bone tissue engineering. However, it is still unknown how well these scaffolds function in terms of biomechanical properties and *in-vivo* bone regeneration. Li et al. [53] evaluated the osteogenic performance of patient-specific 3D printed PEEK scaffolds fabricated using FDM 3D printing technology. They also compared the biomechanical characteristics of PEEK scaffolds with patient-specific 3D printed titanium scaffolds fabricated using selective laser melting (SLM) 3D printing technology. Figure 26 demonstrates the virtual design and production of PEEK and titanium scaffolds made specifically for the patient's maxilla. 3D alveolar bone defects were recreated as shown in Fig. 26(a) along with dentition restoration, implant placement and alveolar bone contour simulations (Figs. 26(b) and 26(c)).

A 3D scaffold was designed based on the recreated bone contour and then patient-specific PEEK and titanium scaffolds were created using FDM and SLM, respectively, as displayed in Figs. 26(d)–26(f). Both scaffolds are shown to have comparable bone ingrowth efficiency and space maintenance capacity in *in-vivo* studies (Figs. 26(j)–26(s)). The work by Li et al. [53] offered early proof that patient-specific PEEK scaffolds had therapeutic promise and could maintain space and promote bone formation in a manner comparable to patient-specific titanium scaffolds. This study offered a basic foundation for the therapeutic application of the non-metallic 3D printed scaffolds in individualized dental bone tissue engineering. However, there are some limitations revealed in this study include first, the design of the PEEK scaffold was not optimized owing to the poor manufacturing precision of FDM. Moreover, the PEEK scaffold's biomechanical performance would vary depending on configuration and pore size. Therefore, more research including mechanical studies and animal experiments is required to determine the ideal internal structural arrangements.

By using the SLM technique, Wang et al. [15] reported 3D printed porous titanium alloy-based scaffolds with a trabecular-like structure and different pore sizes. Figure 27(a) provides a schematic representation of the 3D printing procedures used to create scaffolds that mimic trabecular bone structure. Using the SLM technique and Ti6Al4V as the raw material, each group of scaffolds was produced. The macroscopic pictures of each set of porous Ti6Al4V scaffolds along with CAD models, μCT images, and SEM images are shown in Figs. 27(b)–27(e). According to the *in-vitro* study (upper panel in Fig. 28), the titanium alloy-based scaffolds with a trabecular-like structure showed better *in-vitro* cell growth and differentiation compared with the regular structured titanium alloy-based scaffolds. Additionally, the rabbit tibia bone defect model (upper panel in Fig. 28) was used to test the *in-vivo* performance of the titanium alloy-based scaffolds. The *in-vivo* findings (lower panel in Fig. 28) revealed that the titanium alloy-based scaffolds with a trabecular-like structure had the best potential for bone tissue integration and new bone formation.

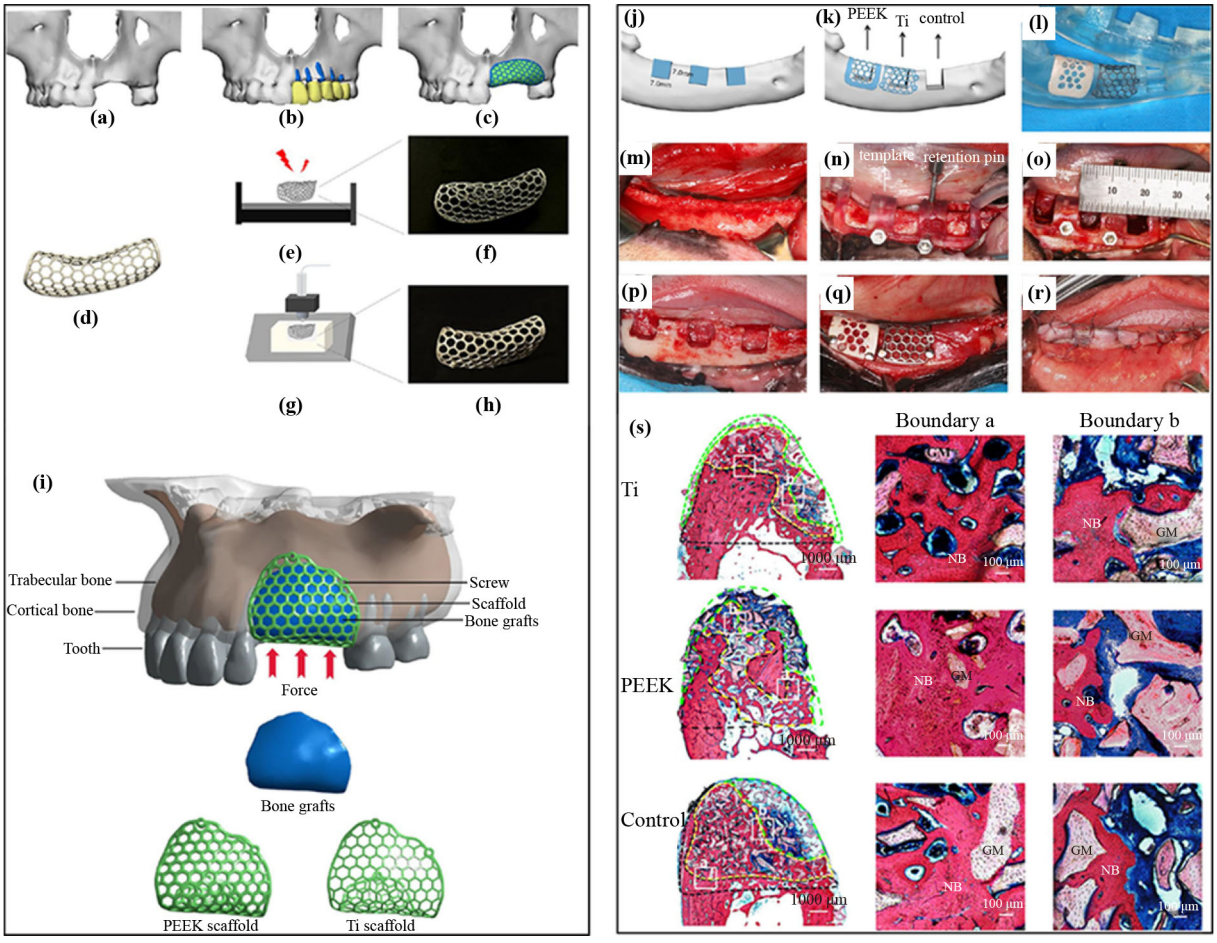

Fig. 26 (**a**)–(**h**) Design and production of PEEK scaffold fabricated using FDM and titanium scaffolds (fabricated by SLM) made specifically for the patient's maxilla. (**i**) Finite element models of PEEK and titanium scaffolds. (**j**)–(**r**) Design and execution of *in-vivo* operation. (**s**) Histological images of implanted PEEK and titanium scaffolds along with control. Pink color refers to new bone. Reproduced with permission from Ref. [53] (Copyright 2022, The American Chemical Society).

5 Conclusions and future perspectives

Traditionally manufactured scaffolds are widely investigated for bone tissue engineering. However, these scaffolds suffer from several drawbacks and unavoidable limitations including non-tunable shape, non-uniform porosity, irregular pore size/pore shape, long processing times and low production reproducibly. 3D printing has recently become a hot area of research and it is now the subject of in-depth study for the production of 3D scaffolds for bone tissue engineering. Actually, the application of 3D printing in the bone tissue engineering is continually expanding. The primary goal of 3D printing in bone tissue engineering is to satisfy the requirements of a patient-specific scaffold with pre-customized and personalized architecture. In addition, printable biomaterials should be biocompatible and processable while yet being cell-friendly and the 3D printing technique should provide precise control over the scaffold production process. The exact control over scaffold exterior form, internal architecture, porosity, pore design, pore size, and pore network interconnectivity that 3D printing techniques can provide is impossible to achieve using conventional methods. 3D printing is a manufacturing technology for printing complex 3D structures through a layer-by-layer additive deposition of a printable material (ink) using 3D digital models created with CAD. By combining 3D printing with modern imaging and CADs, it is possible to quickly and easily create scaffolds with unique and complex shapes. Three of the key benefits of 3D printing technology are the capacity to produce complex structures with low waste and high flexibility. The use of a wide range of 3D printing technologies such as SLA, SLS, FDM, and IJP enabled the production of complex scaffold architecture with highly controlled

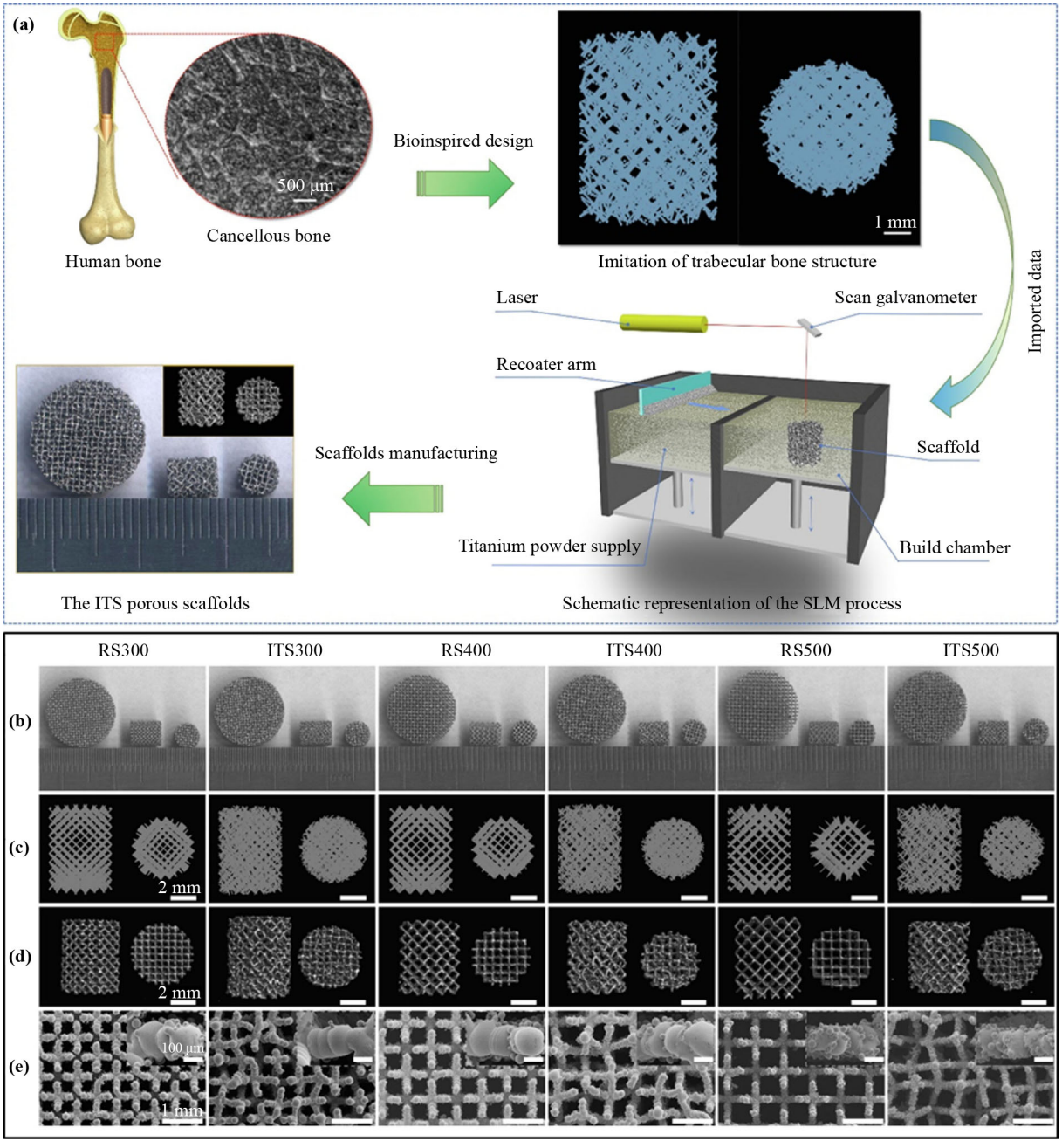

Fig. 27 A schematic representation of (**a**) the 3D-printing procedures used to create scaffolds using SLS, along with (**b**) the macroscopic pictures, (**c**) design models, (**d**) μCT images, and (**e**) SEM images. Reproduced with permission from Ref. [15] (Copyright 2022, Elsevier).

porosity. SLA gives the best resolution and dimensional accuracy when compared across all 3D printing techniques. But there is a problem with the lack of readily available biodegradable photopolymer components. The FDM technique is easy and cheap, but the biomaterial must be formulated into a filament, necessitating a pre-process step that is only applicable to thermoplastic polymers. The SLS technique is costly and offers a good resolution, but because of the high laser intensity, biomaterial may degrade during processing. IJP is a low-cost, low-temperature printing method however low mechanical strength may be seen in the printed green scaffold. As a result, thermal post-processing is required, which causes dimensional error as a result of the shrinkage effect.

Despite the availability of a variety of biomaterials, including ceramics, polymers, and ceramic/polymers composites, 3D printing is still limited by factors

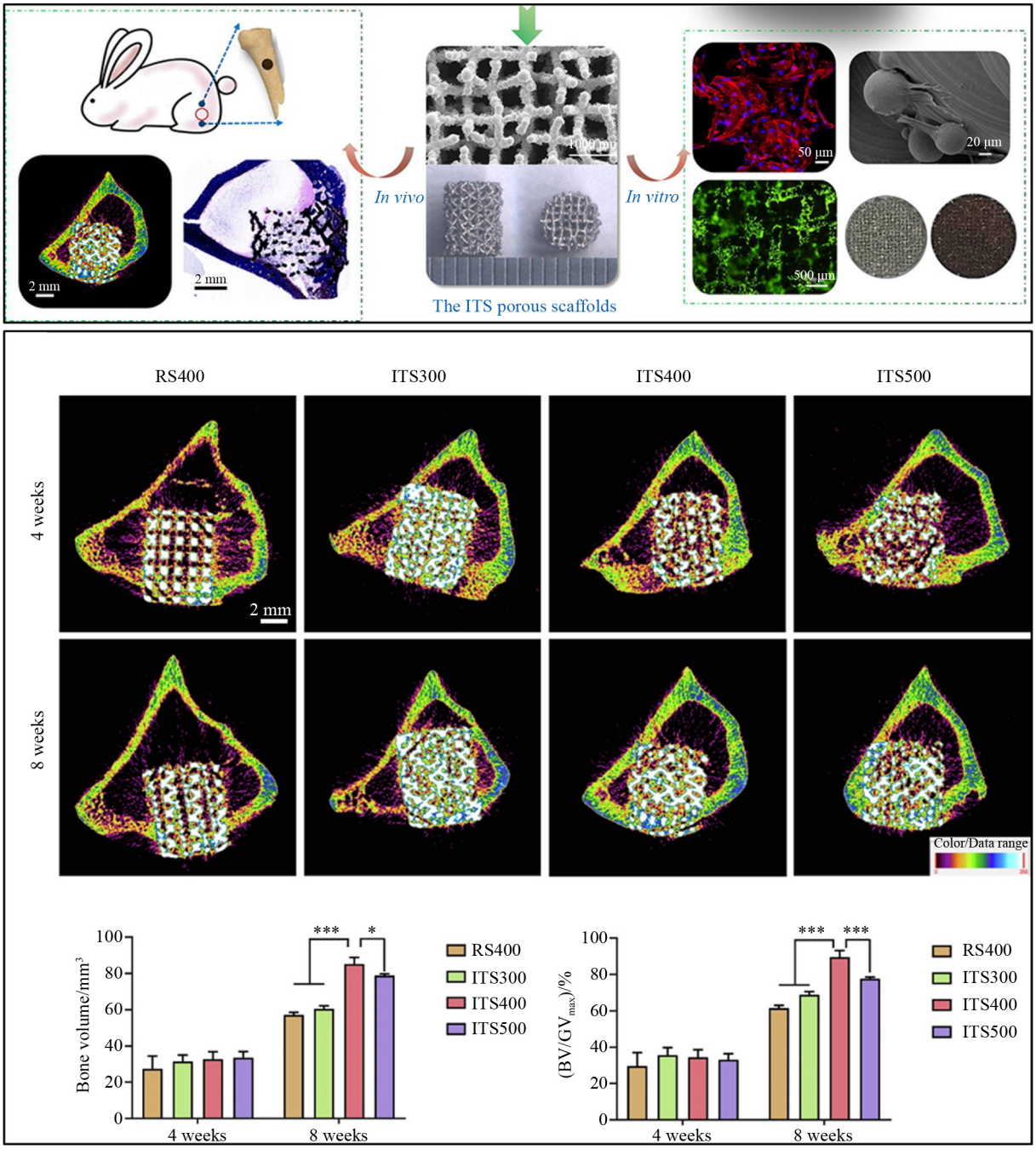

Fig. 28 *In-vivo* animal study of titanium alloy-based scaffolds with a trabecular-like structure (ITS). White: scaffold. Purple: soft tissue. Green, blue, and yellow: new bone tissue. Reproduced with permission from Ref. [15] (Copyright 2022, Elsevier).

including biomaterial ink printability, appropriate mechanical strength, biodegradability, and biocompatibility. For instance, only a few amount of biodegradable polymers is currently available for 3D printing. Therefore, there is an urgent need for research to develop new biomaterials inks with suitable printability and relevant properties that can enable production of 3D printed scaffolds that mimic the native bone tissue in its complex porosity levels, chemical make-up and mechanical properties. Application of 3D printing for bone tissue engineering has been advanced significantly during the last few years owing to fast growing research and it is expected that 3D printing technology will replace conventional manufacturing methods in the near future. While these new developments in 3D printing for bone tissue engineering are encouraging, the development of

patient-specific scaffolds is still progressing slowly. Actually, 3D printing has made a substantial contribution to contemporary biomaterial research and innovation for the goal of fabricating intricate and customized scaffolds with patient-specific requirements. However, it still faces some difficulties and obstacles including resource shortages and regulatory concerns. Additionally, future research should concentrate on more clinical studies using patient-specific 3D printed scaffolds to improve the clinical outcomes for bone tissue engineering. Finally, the challenge of large-scale manufacturing is something that all of the aforementioned 3D printing methods must overcome. The expenses and printing rates of a 3D manufactured product are the two greatest obstacles for large scale production. Because of the high expenses, the SLS has not been used in the biomedical sector, despite its ability to create certain metal scaffolds in relatively low amounts. Additionally, it is anticipated that SLA and FDM 3D printing techniques will achieve large scale manufacture of medical scaffolds for bone tissue engineering in the near future as a result of the growing commercialization and standardization of the biomaterials used in these techniques. Future research efforts should also highly concentrate on creating standardized 3D printable raw biomaterial inks and on enhancing the 3D printing rate, which is anticipated to hasten the large-scale production process.

References

[1] Pina S, Ribeiro V P, Marques C F, et al. Scaffolding strategies for tissue engineering and regenerative medicine applications. Materials, 2019, 12(11): 1824

[2] Sola A, Bertacchini J, D'Avella D, et al. Development of solvent-casting particulate leaching (SCPL) polymer scaffolds as improved three-dimensional supports to mimic the bone marrow niche. Materials Science and Engineering C, 2019, 96: 153–165

[3] Conoscenti G, Schneider T, Stoelzel K, et al. PLLA scaffolds produced by thermally induced phase separation (TIPS) allow human chondrocyte growth and extracellular matrix formation dependent on pore size. Materials Science and Engineering C, 2017, 80: 449–459

[4] Moghadam M Z, Hassanajili S, Esmaeilzadeh F, et al. Formation of porous HPCL/LPCL/HA scaffolds with supercritical CO_2 gas foaming method. Journal of the Mechanical Behavior of Biomedical Materials, 2017, 69: 115–127

[5] Kordjamshidi A, Saber-Samandari S, Ghadiri Nejad M, et al. Preparation of novel porous calcium silicate scaffold loaded by celecoxib drug using freeze drying technique: Fabrication, characterization and simulation. Ceramics International, 2019, 45(11): 14126–14135

[6] Xu X, Ren S, Li L, et al. Biodegradable engineered fiber scaffolds fabricated by electrospinning for periodontal tissue regeneration. Journal of Biomaterials Applications, 2021, 36(1): 55–75

[7] Alagoz A S, Hasirci V. 3D printing of polymeric tissue engineering scaffolds using open-source fused deposition modeling. Emergent Materials, 2020, 3(4): 429–439

[8] Gayer C, Ritter J, Bullemer M, et al. Development of a solvent-free polylactide/calcium carbonate composite for selective laser sintering of bone tissue engineering scaffolds. Materials Science and Engineering C, 2019, 101: 660–673

[9] Liu R, Ma L, Liu H, et al. Effects of pore size on the mechanical and biological properties of stereolithographic 3D printed hap bioceramic scaffold. Ceramics International, 2021, 47(20): 28924–28931

[10] Sun W, Zhang Y, Gregory D A, et al. Patterning the neuronal cells via inkjet printing of self-assembled peptides on silk scaffolds. Progress in Natural Science, 2020, 30(5): 686–696

[11] Alizadeh-Osgouei M, Li Y, Wen C. A comprehensive review of biodegradable synthetic polymer–ceramic composites and their manufacture for biomedical applications. Bioactive Materials, 2018, 4(1): 22–36

[12] Turnbull G, Clarke J, Picard F, et al. 3D bioactive composite scaffolds for bone tissue engineering. Bioactive Materials, 2018, 3(3): 278–314

[13] El-Fiqi A, Park J H. Novel large-volume and highly porous scaffold of poly(ε-caprolactone) microfibers/collagen nanofibers for regenerative medicine. Materials Letters, 2022, 322: 132474

[14] Kirillova A, Yeazel T R, Asheghali D, et al. Fabrication of biomedical scaffolds using biodegradable polymers. Chemical Reviews, 2021, 121(18): 11238–11304

[15] Wang Z, Zhang M, Liu Z, et al. Biomimetic design strategy of complex porous structure based on 3D printing Ti–6Al–4V scaffolds for enhanced osseointegration. Materials & Design, 2022, 218: 110721

[16] Du X, Dehghani M, Alsaadi N, et al. A femoral shape porous scaffold bio-nanocomposite fabricated using 3D printing and freeze-drying technique for orthopedic application. Materials Chemistry and Physics, 2022, 275: 125302

[17] Zhang M, Lin R, Wang X, et al. 3D printing of Haversian bone-mimicking scaffolds for multicellular delivery in bone

regeneration. Science Advances, 2020, 6(12): eaaz6725

[18] Liang H, Wang Y, Chen S, et al. Nano-hydroxyapatite bone scaffolds with different porous structures processed by digital light processing 3D printing. International Journal of Bioprinting, 2022, 8(1): 198–210

[19] Zhu H, Li M, Huang X, et al. 3D printed tricalcium phosphate-bioglass scaffold with gyroid structure enhance bone ingrowth in challenging bone defect treatment. Applied Materials Today, 2021, 25: 101166

[20] Guiney L M, Mansukhani N D, Jakus A E, et al. Three-dimensional printing of cytocompatible, thermally conductive hexagonal boron nitride nanocomposites. Nano Letters, 2018, 18(6): 3488–3493

[21] Mirkhalaf M, Dao A, Schindeler A, et al. Personalized Baghdadite scaffolds: stereolithography, mechanics and *in vivo* testing. Acta Biomaterialia, 2021, 132: 217–226

[22] Mbundi L, Gonzalez-Perez M, Gonzalez-Perez F, et al. Trends in the development of tailored elastin-like recombinamer-based porous biomaterials for soft and hard tissue applications. Frontiers in Materials, 2021, 7: 601795

[23] El-Fiqi A, Kim H W. Nano/micro-structured poly(ε-caprolactone)/gelatin nanofibers with biomimetically-grown hydroxyapatite spherules: high protein adsorption, controlled protein delivery and sustained bioactive ions release designed as a multifunctional bone regenerative membrane. Ceramics International, 2021, 47(14): 19873–19885

[24] Lu X, Wang C, Favier F, et al. Electrospun nanomaterials for supercapacitor electrodes: designed architectures and electrochemical performance. Advanced Energy Materials, 2017, 7(2): 1601301

[25] Kim J J, El-Fiqi A, Kim H W. Synergetic cues of bioactive nanoparticles and nanofibrous structure in bone scaffolds to stimulate osteogenesis and angiogenesis. ACS Applied Materials & Interfaces, 2017, 9(3): 2059–2073

[26] Kim J J, Bang S H, El-Fiqi A, et al. Fabrication of nanofibrous macroporous scaffolds of poly(lactic acid) incorporating bioactive glass nanoparticles by camphene-assisted phase separation. Materials Chemistry and Physics, 2014, 143(3): 1092–1101

[27] El-Fiqi A, Lee J H, Lee E J, et al. Collagen hydrogels incorporated with surface-aminated mesoporous nanobioactive glass: improvement of physicochemical stability and mechanical properties is effective for hard tissue engineering. Acta Biomaterialia, 2013, 9(12): 9508–9521

[28] Jo S B, Erdenebileg U, Dashnyam K, et al. Nano-graphene oxide/polyurethane nanofibers: mechanically flexible and myogenic stimulating matrix for skeletal tissue engineering. Journal of Tissue Engineering, 2020, 11: 2041731419900424

[29] Syed O, Kim J H, Keskin-Erdogan Z, et al. SIS/aligned fibre scaffold designed to meet layered oesophageal tissue complexity and properties. Acta Biomaterialia, 2019, 99: 181–195

[30] El-Fiqi A, Seo S J, Kim H W. Chapter 15: Mineralization of fibers for bone regeneration. In: Aparicio C, Ginebra M P, eds. Biomineralization and Biomaterials — Fundamentals and Applications. Woodhead Publishing, 2015, 443–476

[31] Collins M N, Ren G, Young K, et al. Scaffold fabrication technologies and structure/function properties in bone tissue engineering. Advanced Functional Materials, 2021, 31(21): 2010609

[32] El-Fiqi A, Kim J H, Kim H W. Osteoinductive fibrous scaffolds of biopolymer/mesoporous bioactive glass nanocarriers with excellent bioactivity and long-term delivery of osteogenic drug. ACS Applied Materials & Interfaces, 2015, 7(2): 1140–1152

[33] Buitrago J O, Patel K D, El-Fiqi A, et al. Silk fibroin/collagen protein hybrid cell-encapsulating hydrogels with tunable gelation and improved physical and biological properties. Acta Biomaterialia, 2018, 69: 218–233

[34] Lee J H, Park J H, El-Fiqi A, et al. Biointerface control of electrospun fiber scaffolds for bone regeneration: engineered protein link to mineralized surface. Acta Biomaterialia, 2014, 10(6): 2750–2761

[35] Lim H C, Nam O H, Kim M J, et al. Delivery of dexamethasone from bioactive nanofiber matrices stimulates odontogenesis of human dental pulp cells through integrin/BMP/mTOR signaling pathways. International Journal of Nanomedicine, 2016, 11: 2557–2567

[36] El-Fiqi A, Kim H W. Mesoporous bioactive nanocarriers in electrospun biopolymer fibrous scaffolds designed for sequential drug delivery. RSC Advances, 2014, 4(9): 4444–4452

[37] El-Kady A M, Ali A A, El-Fiqi A. Controlled delivery of therapeutic ions and antibiotic drug of novel alginate-agarose matrix incorporating selenium-modified borosilicate glass designed for chronic wound healing. Journal of Non-Crystalline Solids, 2020, 534: 119889

[38] Kim G H, Park Y D, Lee S Y, et al. Odontogenic stimulation of human dental pulp cells with bioactive nanocomposite fiber. Journal of Biomaterials Applications, 2015, 29(6): 854–866

[39] Liu K, Yan L, Li R, et al. 3D printed personalized nerve guide conduits for precision repair of peripheral nerve defects. Advanced Science, 2022, 9(12): 2103875

[40] Zhang F, Li Z, Xu M, et al. A review of 3D printed porous ceramics. Journal of the European Ceramic Society, 2022, 42(8): 3351–3373

[41] Studart A R, Gonzenbach U T, Tervoort E, et al. Processing

routes to macroporous ceramics: a review. Journal of the American Ceramic Society, 2006, 89(6): 1771–1789

[42] Baino F, Novajra G, Vitale-Brovarone C. Bioceramics and scaffolds: a winning combination for tissue engineering. Frontiers in Bioengineering and Biotechnology, 2015, 3: 202

[43] Kumar M, Sharma V. Additive manufacturing techniques for the fabrication of tissue engineering scaffolds: a review. Rapid Prototyping Journal, 2021, 27(6): 1230–1272

[44] Kanwar S, Vijayavenkataraman S. Design of 3D printed scaffolds for bone tissue engineering: a review. Bioprinting, 2021, 24: e00167

[45] Feng X, Ma L, Liang H, et al. Osteointegration of 3D-printed fully porous polyetheretherketone scaffolds with different pore sizes. ACS Omega, 2020, 5(41): 26655–26666

[46] Soleymani Eil Bakhtiari S, Bakhsheshi-Rad H R, Karbasi S, et al. 3-Dimensional printing of hydrogel-based nanocomposites: a comprehensive review on the technology description, properties, and applications. Advanced Engineering Materials, 2021, 23(10): 2100477

[47] Asadi-Eydivand M, Brown T C, Bagheri A. Raft-mediated 3D printing of "living" materials with tailored hierarchical porosity. ACS Applied Polymer Materials, 2022, 4(7): 4940–4948

[48] Tesavibul P, Felzmann R, Gruber S, et al. Processing of 45S5 Bioglass® by lithography-based additive manufacturing. Materials Letters, 2012, 74: 81–84

[49] Chen Y, Li W, Zhang C, et al. Recent developments of biomaterials for additive manufacturing of bone scaffolds. Advanced Healthcare Materials, 2020, 9(23): 2000724

[50] Bahraminasab M. Challenges on optimization of 3D-printed bone scaffolds. Biomedical Engineering Online, 2020, 19(1): 69

[51] Thavornyutikarn B, Tesavibul P, Sitthiseripratip K, et al. Porous 45S5 Bioglass®-based scaffolds using stereolithography: effect of partial pre-sintering on structural and mechanical properties of scaffolds. Materials Science and Engineering C, 2017, 75: 1281–1288

[52] Germaini M M, Belhabib S, Guessasma S, et al. Additive manufacturing of biomaterials for bone tissue engineering — a critical review of the state of the art and new concepts. Progress in Materials Science, 2022, 130: 100963

[53] Li L, Gao H, Wang C, et al. Assessment of customized alveolar bone augmentation using titanium scaffolds vs polyetheretherketone (PEEK) scaffolds: a comparative study based on 3D printing technology. ACS Biomaterials Science & Engineering, 2022, 8(5): 2028–2039

[54] Challa B T, Gummadi S K, Elhattab K, et al. In-house processing of 3D printable polyetheretherketone (PEEK) filaments and the effect of fused deposition modeling parameters on 3D-printed peek structures. International Journal of Advanced Manufacturing Technology, 2022, 121(3–4): 1675–1688

[55] Distler T, Fournier N, Grünewald A, et al. Polymer–bioactive glass composite filaments for 3D scaffold manufacturing by fused deposition modeling: fabrication and characterization. Frontiers in Bioengineering and Biotechnology, 2020, 8: 552

[56] Zhu H, Monavari M, Zheng K, et al. 3D bioprinting of multifunctional dynamic nanocomposite bioinks incorporating Cu-doped mesoporous bioactive glass nanoparticles for bone tissue engineering. Small, 2022, 18(12): 2104996

[57] Lai J, Wang C, Wang M. 3D printing in biomedical engineering: processes, materials, and applications. Applied Physics Reviews, 2021, 8(2): 021322

[58] Zhang B, Cristescu R, Chrisey D B, et al. Solvent-based extrusion 3D printing for the fabrication of tissue engineering scaffolds. International Journal of Bioprinting, 2020, 6(1): 28–42

[59] Schwab A, Levato R, D'Este M, et al. Printability and shape fidelity of bioinks in 3D bioprinting. Chemical Reviews, 2020, 120(19): 11028–11055

[60] Schwab A, Levato R, D'Este M, et al. Printability and shape fidelity of bioinks in 3D bioprinting. Chemical Reviews, 2020, 120(19): 10850–10877

[61] Li W, Mille L S, Robledo J A, et al. Recent advances in formulating and processing biomaterial inks for vat polymerization-based 3D printing. Advanced Healthcare Materials, 2020, 9(15): 2000156

[62] Pedrero S G, Llamas-Sillero P, Serrano-López J. A multidisciplinary journey towards bone tissue engineering. Materials, 2021, 14(17): 4896

[63] Ibrahim A. Chapter 13: 3D bioprinting bone. In: Thomas D J, Jessop Z M, Whitaker I S, eds. 3D Bioprinting for Reconstructive Surgery — Techniques and Applications. Woodhead Publishing, 2017, 245–275

[64] Vidal L, Kampleitner C, Brennan M Á, et al. Reconstruction of large skeletal defects: current clinical therapeutic strategies and future directions using 3D printing. Frontiers in Bioengineering and Biotechnology, 2020, 8: 61

[65] Grassie K, Khan Y. Chapter 1: Bone tissue engineering. In: Chen Y, ed. Musculoskeletal Tissue Engineering. Elsevier, 2022, 1–40

[66] Maia F R, Bastos A R, Oliveira J M, et al. Recent approaches towards bone tissue engineering. Bone, 2022, 154: 116256

[67] Ranjan R, Kumar D, Kundu M, et al. A critical review on classification of materials used in 3D printing process. Materials Today: Proceedings, 2022, 61: 43–49

[68] Anandhapadman A, Venkateswaran A, Jayaraman H, et al. Advances in 3D printing of composite scaffolds for the repairment of bone tissue associated defects. Biotechnology Progress, 2022, 38(3): e3234

[69] Ramburrun P, Indermun S, Govender M, et al. Research progress of scaffold materials. In: Mozafari M, Sefat F, Atala A, eds. Handbook of Tissue Engineering Scaffolds: Volume One. Woodhead Publishing, 2019, 93–108

[70] Zhang M, Qin C, Wang Y, et al. 3D printing of tree-like scaffolds for innervated bone regeneration. Additive Manufacturing, 2022, 54: 102721

[71] Daguano J K M B, Giora F C, Santos K F, et al. Shear-thinning sacrificial ink for fabrication of biosilicate® osteoconductive scaffolds by material extrusion 3D printing. Materials Chemistry and Physics, 2022, 287: 126286

[72] Pierantozzi D, Scalzone A, Jindal S, et al. 3D printed Sr-containing composite scaffolds: effect of structural design and material formulation towards new strategies for bone tissue engineering. Composites Science and Technology, 2020, 191: 108069

[73] Liu X, Miao Y, Liang H, et al. 3D-printed bioactive ceramic scaffolds with biomimetic micro/nano-HAp surfaces mediated cell fate and promoted bone augmentation of the bone-implant interface *in vivo*. Bioactive Materials, 2022, 12: 120–132

[74] Sun H, Zhang C, Zhang B, et al. 3D printed calcium phosphate scaffolds with controlled release of osteogenic drugs for bone regeneration. Chemical Engineering Journal, 2022, 427: 130961

[75] Shao H, Nian Z, Jing Z, et al. Additive manufacturing of hydroxyapatite bioceramic scaffolds with projection based 3D printing. Chinese Journal of Mechanical Engineering: Additive Manufacturing Frontiers, 2022, 1(2): 100021

[76] Van Hede D, Liang B, Anania S, et al. 3D-printed synthetic hydroxyapatite scaffold with in silico optimized macrostructure enhances bone formation *in vivo*. Advanced Functional Materials, 2022, 32(6): 2105002

[77] Wang M M, Flores R L, Witek L, et al. Dipyridamole-loaded 3D-printed bioceramic scaffolds stimulate pediatric bone regeneration *in vivo* without disruption of craniofacial growth through facial maturity. Scientific Reports, 2019, 9(1): 18439

[78] Kumar A, Kargozar S, Baino F, et al. Additive manufacturing methods for producing hydroxyapatite and hydroxyapatite-based composite scaffolds: a review. Frontiers in Materials, 2019, 6: 313

[79] Chen Y, Chen L, Wang Y, et al. Lithium-containing bioactive glasses enhanced 3D-printed plga scaffolds for bone regeneration in diabetes. Composites Part B: Engineering, 2022, 230: 109550

[80] Nommeots-Nomm A, Lee P D, Jones J R. Direct ink writing of highly bioactive glasses. Journal of the European Ceramic Society, 2018, 38(3): 837–844

[81] Baier R V, Contreras Raggio J I, Giovanetti C M, et al. Shape fidelity, mechanical and biological performance of 3D printed polycaprolactone–bioactive glass composite scaffolds. Biomaterials Advances, 2022, 134: 112540

[82] Bidgoli M R, Alemzadeh I, Tamjid E, et al. Fabrication of hierarchically porous silk fibroin–bioactive glass composite scaffold via indirect 3D printing: effect of particle size on physico-mechanical properties and *in vitro* cellular behavior. Materials Science and Engineering C, 2019, 103: 109688

[83] Dai Q, Li Q, Gao H, et al. 3D printing of Cu-doped bioactive glass composite scaffolds promotes bone regeneration through activating the HIF-1α and TNF-α pathway of hUVECs. Biomaterials Science, 2021, 9(16): 5519–5532

[84] Simorgh S, Alasvand N, Khodadadi M, et al. Additive manufacturing of bioactive glass biomaterials. Methods, 2022, 208: 75–91

[85] Wang S, Gu R, Wang F, et al. 3D-printed PCL/Zn scaffolds for bone regeneration with a dose-dependent effect on osteogenesis and osteoclastogenesis. Materials Today Bio, 2022, 13: 100202

[86] Fallah A, Altunbek M, Bartolo P, et al. 3D printed scaffold design for bone defects with improved mechanical and biological properties. Journal of the Mechanical Behavior of Biomedical Materials, 2022, 134: 105418

[87] Kwon D Y, Kwon J S, Park S H, et al. A computer-designed scaffold for bone regeneration within cranial defect using human dental pulp stem cells. Scientific Reports, 2015, 5(1): 12721

[88] Yan Y, Chen H, Zhang H, et al. Vascularized 3D printed scaffolds for promoting bone regeneration. Biomaterials, 2019, 190–191: 97–110

[89] Seo Lee J, Nah H, Lee D, et al. Immediately implantable extracellular matrix-enriched osteoinductive hydrogel-laden 3D-printed scaffold for promoting vascularized bone regeneration *in vivo*. Materials & Design, 2022, 219: 110801

[90] Su S, Chen W, Zheng M, et al. Facile fabrication of 3D-printed porous Ti6Al4V scaffolds with a Sr-CaP coating for bone regeneration. ACS Omega, 2022, 7(10): 8391–8402

[91] Choi S, Kim J W, Lee S, et al. Mechanical and biocompatibility properties of sintered titanium powder for mimetic 3D-printed bone scaffolds. ACS Omega, 2022, 7(12): 10340–10346

[92] Zhang Y, Sun N, Zhu M, et al. The contribution of pore size and porosity of 3D printed porous titanium scaffolds to osteogenesis. Biomaterials Advances, 2022, 133: 112651

[93] Yin C, Zhang T, Wei Q, et al. Surface treatment of 3D printed porous Ti6Al4V implants by ultraviolet photofunctionalization

for improved osseointegration. Bioactive Materials, 2022, 7: 26–38

[94] Liu K, Wang J, Fang S, et al. Effect of polycaprolactone impregnation on the properties of calcium silicate scaffolds fabricated by 3D printing. Materials & Design, 2022, 220: 110856

[95] Nie R, Sun Y, Lv H, et al. 3D printing of MXene composite hydrogel scaffolds for photothermal antibacterial activity and bone regeneration in infected bone defect models. Nanoscale, 2022, 14(22): 8112–8129

[96] Wang C, Meng C, Zhang Z, et al. 3D printing of polycaprolactone/bioactive glass composite scaffolds for *in situ* bone repair. Ceramics International, 2022, 48(6): 7491–7499

[97] Oliveira R L M S, Alves A P N, Barbosa L, et al. 3D printing of bioactive glass S53P4/sodium alginate sintering-free scaffolds. Bioprinting, 2022, 27: e00226

[98] Pant S, Thomas S, Loganathan S, et al. 3D bioprinted poly(lactic acid)/mesoporous bioactive glass based biomimetic scaffold with rapid apatite crystallization and *in-vitro* cytocompatability for bone tissue engineering. International Journal of Biological Macromolecules, 2022, 217: 979–997

[99] Richter R F, Ahlfeld T, Gelinsky M, et al. Composites consisting of calcium phosphate cements and mesoporous bioactive glasses as a 3D plottable drug delivery system. Acta Biomaterialia, 2023, 156: 146–157

[100] Monavari M, Homaeigohar S, Fuentes-Chandía M, et al. 3D printing of alginate dialdehyde-gelatin (ADA-GEL) hydrogels incorporating phytotherapeutic icariin loaded mesoporous SiO_2–CaO nanoparticles for bone tissue engineering. Materials Science and Engineering C, 2021, 131: 112470

[101] Sahmani S, Khandan A, Esmaeili S, et al. Calcium phosphate–PLA scaffolds fabricated by fused deposition modeling technique for bone tissue applications: fabrication, characterization and simulation. Ceramics International, 2020, 46(2): 2447–2456

[102] Zou L, Hu L, Pan P, et al. Icariin-releasing 3D printed scaffold for bone regeneration. Composites Part B: Engineering, 2022, 232: 109625

[103] Han S H, Lee J, Lee K M, et al. Enhanced healing of rat calvarial defects with 3D printed calcium-deficient hydroxyapatite/collagen/bone morphogenetic protein 2 scaffolds. Journal of the Mechanical Behavior of Biomedical Materials, 2020, 108: 103782

[104] Saranti A, Tiron-Stathopoulos A, Papaioannou L, et al. 3D-printed bioactive scaffolds for bone regeneration bearing carbon dots for bioimaging purposes. Smart Materials in Medicine, 2022, 3: 12–19

[105] Lee J, Kim D, Jang C H, et al. Highly elastic 3D-printed gelatin/HA/placental-extract scaffolds for bone tissue engineering. Theranostics, 2022, 12(9): 4051–4066

[106] Ha Y, Ma X, Li S, et al. Bone microenvironment-mimetic scaffolds with hierarchical microstructure for enhanced vascularization and bone regeneration. Advanced Functional Materials, 2022, 32(20): 2200011

[107] Zhang J, Tong D, Song H, et al. Osteoimmunity-regulating biomimetically hierarchical scaffold for augmented bone regeneration. Advanced Materials, 2022, 34(36): 2202044

[108] Cao C, Huang P, Prasopthum A, et al. Characterisation of bone regeneration in 3D printed ductile PCL/PEG/hydroxyapatite scaffolds with high ceramic microparticle concentrations. Biomaterials Science, 2021, 10(1): 138–152

[109] Zhao S, Xie K, Guo Y, et al. Fabrication and biological activity of 3D-printed polycaprolactone/magnesium porous scaffolds for critical size bone defect repair. ACS Biomaterials Science & Engineering, 2020, 6(9): 5120–5131

[110] Baino F, Magnaterra G, Fiume E, et al. Digital light processing stereolithography of hydroxyapatite scaffolds with bone-like architecture, permeability, and mechanical properties. Journal of the American Ceramic Society, 2022, 105(3): 1648–1657

[111] Chaudhary R, Fabbri P, Leoni E, et al. Additive manufacturing by digital light processing: a review. Progress in Additive Manufacturing, 2022

[112] Han H H, Shim J H, Lee H, et al. Reconstruction of complex maxillary defects using patient-specific 3D-printed biodegradable scaffolds. Plastic and Reconstructive Surgery - Global Open, 2018, 6(11): e1975

[113] Jakus A E, Rutz A L, Jordan S W, et al. Hyperelastic “bone”: a highly versatile, growth factor-free, osteoregenerative, scalable, and surgically friendly biomaterial. Science Translational Medicine, 2016, 8(358): 358ra127

[114] Lee S H, Lee K G, Hwang J H, et al. Evaluation of mechanical strength and bone regeneration ability of 3D printed kagome-structure scaffold using rabbit calvarial defect model. Materials Science and Engineering C, 2019, 98: 949–959

[115] Wu R, Li Y, Shen M, et al. Bone tissue regeneration: the role of finely tuned pore architecture of bioactive scaffolds before clinical translation. Bioactive Materials, 2021, 6(5): 1242–1254

[116] Remy M T, Akkouch A, He L, et al. Rat calvarial bone regeneration by 3D-printed β-tricalcium phosphate incorporating microRNA-200C. ACS Biomaterials Science & Engineering, 2021, 7(9): 4521–4534

[117] Zhang Q, Ma L, Ji X, et al. High-strength hydroxyapatite scaffolds with minimal surface macrostructures for load-bearing bone regeneration. Advanced Functional Materials, 2022, 32(33): 2204182

[118] Raymond Y, Lehmann C, Thorel E, et al. 3D printing with star-

shaped strands: a new approach to enhance *in vivo* bone regeneration. Biomaterials Advances, 2022, 137: 212807

[119] Xu C, Wu F, Yang J, et al. 3D printed long-term structurally stable bioceramic dome scaffolds with controllable biodegradation favorable for guided bone regeneration. Chemical Engineering Journal, 2022, 450: 138003

[120] Zhang B, Gui X, Song P, et al. Three-dimensional printing of large-scale, high-resolution bioceramics with micronano inner porosity and customized surface characterization design for bone regeneration. ACS Applied Materials & Interfaces, 2022, 14(7): 8804–8815

[121] Ahn J H, Kim J, Han G, et al. 3D-printed biodegradable composite scaffolds with significantly enhanced mechanical properties via the combination of binder jetting and capillary rise infiltration process. Additive Manufacturing, 2021, 41: 101988

[122] Putra N E, Borg K G N, Diaz-Payno P J, et al. Additive manufacturing of bioactive and biodegradable porous iron-akermanite composites for bone regeneration. Acta Biomaterialia, 2022, 148: 355–373

[123] Wei J, Yan Y, Gao J, et al. 3D-printed hydroxyapatite microspheres reinforced PLGA scaffolds for bone regeneration. Biomaterials Advances, 2022, 133: 112618

[124] Zhao X, Wang S, Wang F, et al. 3D-printed Mg-1Ca/polycaprolactone composite scaffolds with promoted bone regeneration. Journal of Magnesium and Alloys, 2022, in press

[125] Wang Z, Lin D, Wang M, et al. Seamless route of self-assembly and 3D printing to fabricate hierarchical mesoporous bioactive glass scaffold for customized bone regeneration with enhanced efficacy. Chemical Engineering Journal, 2022, 446: 137270

[126] Wang X, Zhai D, Yao X, et al. 3D printing of pink bioceramic scaffolds for bone tumor tissue therapy. Applied Materials Today, 2022, 27: 101443

[127] Dong D, Su H, Li X, et al. Microstructures and mechanical properties of biphasic calcium phosphate bioceramics fabricated by SLA 3D printing. Journal of Manufacturing Processes, 2022, 81: 433–443

[128] Martins M I, Rodrigues M A, Lopes M A, et al. Preparation and characterization of customized bone grafting hydroxyapatite models obtained by digital light processing 3D printing. Journal of Materials Research, 2022, 37(3): 784–795

[129] Pant S, Subramanian S, Thomas S, et al. Tailoring of mesoporous bioactive glass composite scaffold via thermal extrusion based 3D bioprinting and scrutiny on bone tissue engineering characteristics. Microporous and Mesoporous Materials, 2022, 341: 112104

[130] Kolan K C R, Huang Y W, Semon J A, et al. 3D-printed biomimetic bioactive glass scaffolds for bone regeneration in rat calvarial defects. International Journal of Bioprinting, 2020, 6(2): 274